Neurobiology of Disease

Autophagy-Dependent Rhodopsin Degradation Prevents Retinal Degeneration in *Drosophila*

Ryosuke Midorikawa,[1,5] Miki Yamamoto-Hino,[1] Wakae Awano,[2] Yoshimi Hinohara,[3] Emiko Suzuki,[4] Ryu Ueda,[5] and Satoshi Goto[1,2]

[1]Research Group of Glycobiology and Glycotechnology, [2]Mutant Flies Laboratory, [3]Biomolecular Structure Analysis Laboratory, Mitsubishi-Kagaku Institute of Life Sciences, Machida 194-8511, Japan, and [4]Gene Network Laboratory and [5]Invertebrate Genetics Laboratory, National Institute of Genetics, Mishima, Shizuoka 411-8540, Japan

Recent studies have demonstrated protective roles for autophagy in various neurodegenerative disorders, including the polyglutamine diseases; however, the role of autophagy in retinal degeneration has remained unclear. Accumulation of activated rhodopsin in some *Drosophila* mutants leads to retinal degeneration, and although it is known that activated rhodopsin is degraded in endosomal pathways in normal photoreceptor cells, the contribution of autophagy to rhodopsin regulation has remained elusive. This study reveals that activated rhodopsin is degraded by autophagy in collaboration with endosomal pathways to prevent retinal degeneration. Light-dependent retinal degeneration in the *Drosophila* visual system is caused by the knockdown or mutation of autophagy-essential components, such as autophagy-related protein 7 and 8 (*atg-7*/*atg-8*), or genes essential for PE (phosphatidylethanolamine) biogenesis and autophagosome formation, including Phosphatidylserine decarboxylase (*Psd*) and CDP-ethanolamine:diacylglycerol ethanolaminephosphotransferase (*Ept*). The knockdown of *atg-7/8* or *Psd/Ept* produced an increase in the amount of rhodopsin localized to Rab7-positive late endosomes. This rhodopsin accumulation, followed by retinal degeneration, was suppressed by overexpression of Rab7, which accelerated the endosomal degradation pathway. These results indicate a degree of cross talk between the autophagic and endosomal/lysosomal pathways. Importantly, a reduction in rhodopsin levels rescued *Psd* knockdown-induced retinal degeneration. Additionally, the *Psd* knockdown-induced retinal degeneration phenotype was enhanced by *Ppt1* inactivation, which causes infantile neuronal ceroid lipofuscinosis, implying that autophagy plays a significant role in its pathogenesis. Collectively, the current data reveal that autophagy suppresses light-dependent retinal degeneration in collaboration with the endosomal degradation pathway and that rhodopsin is a key substrate for autophagic degradation in this context.

Introduction

Inherited retinal degenerative disorders are pathologically and genetically heterogeneous (Hartong et al., 2006; Michaelides et al., 2006) and are characterized by the premature and progressive death of rod and cone photoreceptors. Several genes are involved in retinal diseases in humans and in animal models (Michaelides et al., 2006; Knust, 2007; Karan et al., 2008), and, of these, the *rhodopsin* gene is most frequently mutated. Approximately 25% of the autosomal dominant retinitis pigmentosa cases in humans result from various mutations of the *rhodopsin* gene; thus, understanding rhodopsin regulation will further our knowledge of retinal disease pathogenesis.

In normal photoreceptors, rhodopsin is transported through early and late endosomes and multivesicular bodies (MVBs) before delivery to lysosomes for degradation (Alloway et al., 2000; Xu et al., 2004; Acharya et al., 2008; Chinchore et al., 2009). Defects in genes involved in this lysosomal trafficking pathway, such as Sunglasses (*Sun*) (Xu et al., 2004), or the vacuolar protein sorting (*vps*) mutants, including *carnation/vps33* and *light/vps41* (Chinchore et al., 2009), result in retinal degeneration in *Drosophila*, attributable to the aberrant accumulation of rhodopsin. Thus, efficient rhodopsin degradation appears to be crucial for the viability of photoreceptor cells. However, it is still unclear whether rhodopsin degradation is controlled solely by the lysosomal pathway or whether other mechanisms, such as autophagy, are also involved.

The autophagy pathway mediates the degradation of cytoplasmic proteins, protein aggregates, and organelles on nutrient starvation (Todde et al., 2009). These cell materials are enclosed by a double-membrane structure, the autophagosome, which fuses with endosomes, MVBs, or lysosomes to enable their degradation. Autophagosome formation requires the Atg8-PE conjugate, a product of ubiquitin-like conjugation reactions, in which the ubiquitin-like protein, Atg8, is added to phosphatidylethanolamine (PE), a plasma membrane lipid component, by Atg7 and Atg3 (which function like E1 and E2 enzymes, respectively). PE is synthesized by phosphatidylserine decarboxylase (Psd) and CDP-ethanolamine:diacylglycerol ethanolaminephosphotrans-

Received April 21, 2010; accepted June 12, 2010.

This work was supported by Ministry of Education, Culture, Sports, Science, and Technology of Japan Grant-in-Aid 60280575 (S.G.) and National Institute of Genetics Cooperative Research Program Grants-in-Aid 2008-A69 and 2009-A54 (S.G., E.S.). We thank Drs. R. L. Glaser, A. Nakamura, S. Munro, and T. P. Neufeld for providing reagents.

Correspondence should be addressed to Satoshi Goto, Department of Physiology, School of Medicine, Keio University, 35 Shinanomachi, Shinjuku-ku, Tokyo 160-8582, Japan. E-mail: sgoto@a7.keio.jp.

M. Yamamoto-Hino's present address: Department of Physiology, School of Medicine, Keio University, 35 Shinanomachi, Shinjuku-ku, Tokyo 160-8582, Japan.

DOI:10.1523/JNEUROSCI.2061-10.2010

 0270-6474/10/3010703-17$15.00/0

ferase (Ept) in mitochondria and endoplasmic reticulum (ER), respectively. Although the yeast *Psd* mutation reduces Atg8p recruitment to the pre-autophagosomal structure (Nebauer et al., 2007), there is no evidence that Psd is required for autophagy in higher organisms.

Previous studies have shown that autophagy plays a neuroprotective role in the CNS. Knock-out mice lacking Atg5 or Atg7, and the *Drosophila atg7* mutant display neuronal degeneration in aged animal brains (Hara et al., 2006; Komatsu et al., 2006; Juhász et al., 2007), probably because of the accumulation of toxic oligomers or large aggregates of soluble, misfolded proteins. Additionally, autophagy inactivation enhances neurodegeneration caused by polyglutamine-containing proteins such as Huntingtin. Although the ubiquitin–proteasome pathway normally degrades these cytoplasmic, misfolded proteins, there is evidence that autophagy acts as a compensatory degradation pathway when the ubiquitin–proteasome pathway is impaired (Pandey et al., 2007). However, it is unclear whether autophagy also compensates for the endosomal/lysosomal pathway during membrane protein degradation.

This study provides the first evidence that degradation of the major rhodopsin, Rhodopsin 1 (Rh1), occurs via cross talk between the autophagy and endosomal degradation pathways, and that autophagy acts as a compensatory pathway when the endosomal/lysosomal pathway is impaired.

Materials and Methods

Drosophila *strains.* The *Drosophila* strains used in this study included the following: *GMR*-GAL4, *UAS-gfp*-RNAi, *UAS-Psd*-RNA#1, *UAS-Psd*-RNAi#2, *UAS-fab1*-RNAi, *UAS-Ept*-RNAi#1, *UAS-Ept*-RNAi#2, *UAS-cpt*-RNAi, *UAS-ptdss1*-RNAi, *UAS-atg8a*-RNAi, *UAS-atg7*-RNAi, *UAS-Ppt1*-RNAi, *y1w67c23 P{EPgy2}CG5991EY03559* (*UAS-Psd*), *w-*, *CS*, y^1 *P{SUPor-P}Atg8a*^{KG07569}*/FM7c*, *w y hs-gfp-atg8b*, *ninaE-atg1-myc;ninaE-atg1-myc*, *UAS-atg6-myc*, *tublin-yfp-rab7*, *w Df(1)446-20*, and *w Ppt1S77F*. The *UAS-Psd*-RNAi#2, *UAS-Ept*-RNAi#2, *UAS-atg8a*-RNAi, and *UAS-Ppt1*-RNAi strains were purchased from the Vienna *Drosophila* RNAi Center (Vienna, Austria). *UAS-Psd* and y^1 *P{SUPor-P}Atg8a*^{KG07569}*/FM7c* flies were purchased from the Bloomington *Drosophila* Stock Center (Indiana University, Bloomington, IN), and *w y hs-gfp-atg8b* and *UAS-atg6-myc* were kindly provided by Dr. Thomas P. Neufeld (University of Minnesota, Minneapolis, MN). The *ninaE-atg1-myc* and *tublin-yfp-rab7* flies were a kind gift from Dr. Bruce A. Edgar (Basic Sciences Division, Fred Hutchinson Cancer Research, Seattle, WA) and Dr. Suzanne Eaton (Max Planck Institute of Molecular Cell Biology and Genetics, Dresden, Germany), respectively. The *w Df(1)446-20* and *w Ppt1S77F* flies were a kind gift from Dr. Robert L. Glaser (New York State Department of Health, Albany, NY). The targeted sites of each *UAS*-RNAi line were as follows (number indicates the distance from the start codon): *UAS-Psd*-RNAi#1, 2-503; *UAS-Psd*-RNAi#2, 751-1145; *UAS-fab1*-RNAi, 532-1031; *UAS-Ept*-RNAi#1, 13-512; *UAS-Ept*-RNAi#2, 963-1222; *UAS-cpt*-RNAi, 555-1045; *UAS-ptdss1*-RNAi, 366-865; *UAS-atg8a*-RNAi, 55-354; *UAS-atg7*-RNAi, 201-700; and *UAS-Ppt1*-RNAi, 90-399. All of the 19-mers in the targeting sequences were compared with the other targeting sequences using dsCheck (Naito et al., 2005).

Antibodies. Rhodopsin 1 and Chaoptin mouse monoclonal antibodies and a DE-cadherin rat monoclonal antibody were obtained from the Developmental Studies Hybridoma Bank (University of Iowa, Iowa City, IA). Rat anti-α-tubulin polyclonal antibodies were purchased from Oxford Biotechnology. Rabbit anti-Myc polyclonal antibodies (A-14) and mouse anti-green fluorescent protein (GFP) monoclonal antibodies (B-2) were purchased from Santa Cruz Biotechnology. Rabbit anti-Rab7 polyclonal antibodies and rabbit anti-Arl8 polyclonal antibodies were a kind gift from Dr. Akira Nakamura (Riken CDB, Kobe, Japan) and Dr. Sean Munro (Medical Research Council–Laboratory of Molecular Biology, Cambridge, UK), respectively. Rabbit anti-GM130 antibodies were produced as previously described (Yano et al., 2005).

Reverse transcription–PCR. Before the extraction of total RNA using the three methods described below, flies were reared in the dark at 27°C. Method A was as follows: The extraction of total RNA and preparation of cDNA from retinal slices was performed using a Power SYBR Green Cells-to-CTTM kit (Ambion). Briefly, 10 retinal slices were collected from adult flies by carefully peeling the compound eyes from the adult heads using tweezers and suspending them in 50 μl of lysis solution with DNaseI. To produce cDNA, 10 μl of the resulting lysate was added to 40 μl of RT MasterMix and incubated at 37°C for 60 min, and then at 95°C for 5 min. An aliquot of 0.5–5 μl of the cDNA solution and specific oligonucleotide primer pairs was then added to the reaction mixture with TaKaRa Ex Taq (TaKaRa) and PCR was performed according to the following program for 33–38 cycles: 94°C for 30 s, 58°C for 30 s, and 72°C for 1 min. The volume of cDNA solution was normalized using control (*gapdh*) bands between samples of knockdown flies and control (*gfp*-RNAi) flies. Method B was as follows: Retinal slices were collected from 100 adult flies by excising the compound eyes followed by the removal of adherent brains. Total RNA was then extracted using an RNeasy Mini Kit (QIAGEN), and the purity of the samples and RNA content was measured using a UV photometer. An aliquot of 140 ng of total RNA was reverse transcribed using SuperScript III Reverse Transcriptase (Invitrogen) and oligo-dT primers in a final volume of 25 μl. This reaction was used as a template for subsequent PCR. Amplifications were performed using the program described above for 31–37 cycles. Method C was as follows: Total RNA from 50 adult fly heads was prepared as described in method B, cDNA was synthesized from 500 ng of total RNA, and PCR was performed for 31 cycles also as described in method B. The sequences of the primers were as follows: *Psd* forward primer-1 (F-1), 5′-ATGGATGCCGATCTGAAGAC-3′; *Psd* reverse primer-1 (R-1), 5′-GGTGCTGCCCATATTGAACT-3′; *Psd* forward primer-2 (F-2), 5′-GGCAATCTCAGACAGGTGGT-3′; *Psd* reverse primer-2 (R-2), 5′-GCAGACTGGGAGGCAAGTAG-3′; *Ept* forward primer, 5′-ATGGATGCCGATCTGAAGAC-3′; *Ept* reverse primer, 5′-GGTGCTGCCCATATTGAACT-3′; *atg8a* forward primer, 5′-ATTGAGGAAAACCGCAGGA-3′; *atg8a* reverse primer, 5′-GCATTCGCACGGATCAATTA-3′; *ptdss1* forward primer, 5′-ATCCACCACAACGGGTAAAA-3′; *ptdss1* reverse primer, 5′-AACCGCGAGGTAGACAAATG-3′; *fab1* forward primer, 5′-CAGCAATCAGCAAGGTGAAA-3′; *fab1* reverse primer, 5′-CCAAGTACCAAGACGCCATT-3′; *cpt* forward primer, 5′-ACGAGCTTCCTCAGCGTCTA-3′; *cpt* reverse primer, 5′-GCTTCGAAACCCCAATCATA-3′; *atg7* forward primer, 5′-TGACCCGGTTCTTTGTTCTC-3′; *atg7* reverse primer, 5′-CTTTGGCTAAGATCGCAAGC-3′; *gapdh* forward primer, 5′-ATCGTCGAGGGTCTGATGAC-3′; and *gapdh* reverse primer, 5′-ACCGAACTCGTTGTCGTACC-3′. The *Psd* F-1/*Psd* R-1 and *Psd* F-2/*Psd* R-2 primer pairs were used for reverse transcription–PCR analysis of *Psd*-RNAi#1 flies and *Psd*-RNAi#2 flies, respectively.

Immunohistochemistry. Immunolabeling of dissected *Drosophila* retinas was performed as follows, and eight to nine flies were quantified in each genotype: adult heads were dissected and sliced in half in fixation buffer [2% paraformaldehyde (PFA), 0.1% Triton X-100 in PBS, or 4% PFA, 0.06% Triton X-100 in PBS]. These half-heads were then placed on ice for 30 min in fixation buffer, and retinal slices were prepared by cutting compound eyes horizontally using dissecting scissors (Vannas Dissecting; World Precision Instruments). Dissected retinas were then fixed in fixation buffer on ice for 30 min and incubated with primary antibodies in blocking buffer (0.1% BSA, 0.1% Triton X-100 in PBS) at room temperature for 2 h. This was followed by incubation with fluorescent-labeled secondary antibodies (Alx-488/Alx-546-conjugated anti-mouse/rat/rabbit IgG; Invitrogen; or anti-mouse IgG Cy5-conjugate; Millipore Bioscience Research Reagents) and Alx-633-conjugated phalloidin (Molecular Probes) in blocking buffer at room temperature for 2 h. The fluorescently labeled slices were transferred onto slides, mounted in 20 μl of 70% glycerol in PBS using an 18×18 mm^2 coverslip and a spacer between the coverslip and slide, and analyzed using a confocal microscope (FluoView FV500; Olympus) equipped with an UPlanApo 100×/1.35 oil-immersion objective. Image processing and analysis were performed with a FluoView FV500 confocal laser-scanning microscope (Olympus) and Adobe Photoshop CS.

Transmission electron microscopy. Drosophila heads were cut longitudinally, fixed in a mixture of 2% PFA and 2% glutaraldehyde in 0.1 M cacodylate buffer, pH 7.4, at room temperature for several hours, washed with 8% sucrose in 0.1 M cacodylate buffer, and then postfixed with 1% osmium tetroxide in 0.1 M cacodylate buffer for 2 h at 4°C. After several

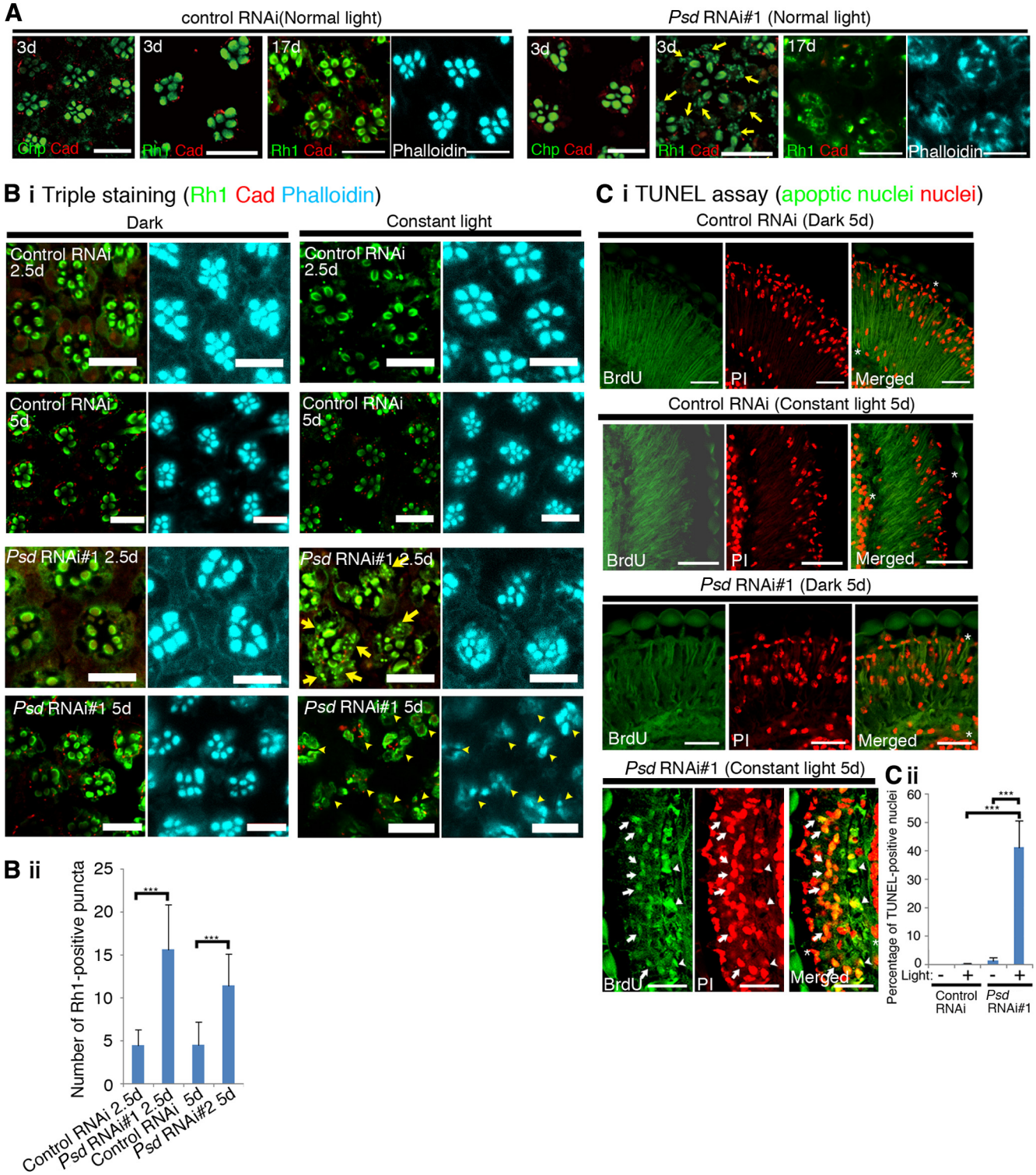

Figure 1. A *Psd* knockdown in *Drosophila* causes light-dependent retinal degeneration after intracellular Rh1 accumulation. ***A***, Immunolabeling of the dissected retinas of control (*gfp*-RNAi) and *Psd*-RNAi#1 flies reared under normal light exposure (NL) (30∼300 lux) for 3 or 17 d. The dissected retinas were immunolabeled with antibodies as indicated in each panel. In the flies reared for 3 d, abnormal Rh1 accumulation was found in the photoreceptors of the *Psd*-RNAi#1 variants (arrows). In the flies reared for 17 d, most of the rhabdomeres (labeled with phalloidin) were lost in the retinas of the *Psd*-RNAi#1 flies. Scale bar, 10 μm. ***B***, Knockdown of *Psd* causes light-dependent ommatidial degeneration. ***Bi***, Dissected retinas from dark-reared or light-exposed flies were triply stained (Rh1, Cad, and phalloidin). A large number of Rh1-positive puncta (arrows) were found in the photoreceptors of *Psd*-RNAi#1 flies after light exposure. Disrupted ommatidia (showing partial or complete loss of a phalloidin-positive rhabdomere; arrowheads) were found after light exposure for 5 d. Scale bar, 10 μm. ***Bii***, Statistical analysis of Rh1-positive puncta after light exposure. The number of Rh1-positive puncta per ommatidium was counted for 150 ommatidia in two independent experiments. The values shown are the mean ± SD. $^{***}p < 0.001$, *t* test. ***C***, A *Psd* knockdown causes light-dependent retinal cell death. ***Ci***, *gfp*-RNAi and *Psd*-RNAi#1 flies were reared under dark or light conditions as indicated in each panel, and a TUNEL assay was performed. In the retinas of light-exposed *Psd*-RNAi#1 flies, TUNEL-positive nuclei were found near the apical surface (arrows) and near to the retinal floor (arrowheads). Scale bars, 20 μm. ***Cii***, Statistical analysis of the TUNEL-positive nuclei shown in ***Ci***. The percentage of TUNEL-positive nuclei located from the apical surface to the retinal floor (indicated by the asterisks in the merged images) is shown. Each value was calculated from 16 frozen sections taken from eight flies. The values shown are the mean ± SD. $^{***}p < 0.001$, *t* test. BrdU, 5-Bromodeoxyuridine; PI, propidium iodide.

washes in distilled water, the specimens were stained with 0.5% aqueous uranyl acetate for 1 h, dehydrated with ethanol, and embedded in Epon 812. Ultrathin sections were cut with an ultramicrotome (Ultracut UCT; Leica), collected on copper slot grids, stained with uranyl acetate/lead citrate, and observed using a transmission electron microscope (JEM-1230; JEOL).

Immuno-electron microscopy. *Drosophila* heads were cut longitudinally, fixed in PLP fixation buffer (4% PFA, 10 mM $NaIO_4$, 75 mM lysine, 37.5 mM phosphate buffer, pH 7.4) at room temperature for 1 h, and incubated at 4°C with 10% sucrose–PBS for 30 min, 20% sucrose–PBS for 1 h, and 30% sucrose–PBS overnight. *Drosophila* heads were then embedded in OCT compound, and 10 μm sections were cut using a cryostat (HM500-OM; Carl Zeiss), blocked with blocking buffer (0.1% saponin, 5% normal goat serum, PBS, pH 7.4) at room temperature for 30 min, immunolabeled with mouse anti-GFP monoclonal antibodies in blocking buffer at 4°C overnight, washed with PBS, and then incubated with secondary antibodies (biotin-conjugated goat anti-mouse antibodies) in blocking buffer at 4°C overnight. The avidin–biotin peroxidase method (Vectastain Elite ABC kit; Vector Laboratories) was used to detect GFP-Atg8b immunoreactivity. The tissue was then washed with PBS at 4°C and incubated with 0.05% diaminobenzidine (DAB) in PBS at room temperature for 30 min, and the peroxidase reaction was developed in 0.05% DAB and 0.03% H_2O_2 for 5 min. At this point, the immunolabeled sections were also analyzed using differential interference contrast microscopy (see Fig. 5*B*). For electron microscopy, the developed slices were washed with PBS, postfixed with 2% OsO4, 0.1 M phosphate buffer, pH 7.4, at room temperature for 1 h, washed with H_2O, dehydrated in a graded ethanol series, and embedded in Epon 812. Ultrathin sections were cut and examined under an electron microscope.

MitoTracker labeling. Ommatidia were isolated from adult *Drosophila* heads essentially as described previously (Hardie, 1991). For MitoTracker labeling, isolated ommatidia were incubated with 100 nM MitoTracker Red CMXRos (Invitrogen) in Schneider's medium at room temperature for 30 min, washed with PBS, incubated again with Schneider's medium at room temperature for 30 min, and fixed with 4% PFA in PBS at 37°C for 20 min. The ommatidia were then washed with PBS, mounted in PBS containing TOPRO3 (Molecular Probes), and analyzed using a confocal microscope as described above.

Immunoblotting. Adult fly heads were homogenized in lysis buffer [20 mM Tris-HCl, pH 7.4, 0.15 M NaCl, 1% Triton X-100, 0.5% DOC (sodium deoxycholate), and 0.1% SDS containing a protease inhibitor mixture; Roche Diagnostics], sonicated, and centrifuged at 15,000 rpm at 4°C for 20 min. The supernatant was collected as the adult head lysate. These lysates were immunoblotted with mouse anti-Rh1 or rat anti-α-tubulin primary antibodies followed by HRP-conjugated anti-mouse/rat antibodies (Pierce). Blots were developed using SuperSignal West Pico Chemiluminescent Substrate (Pierce).

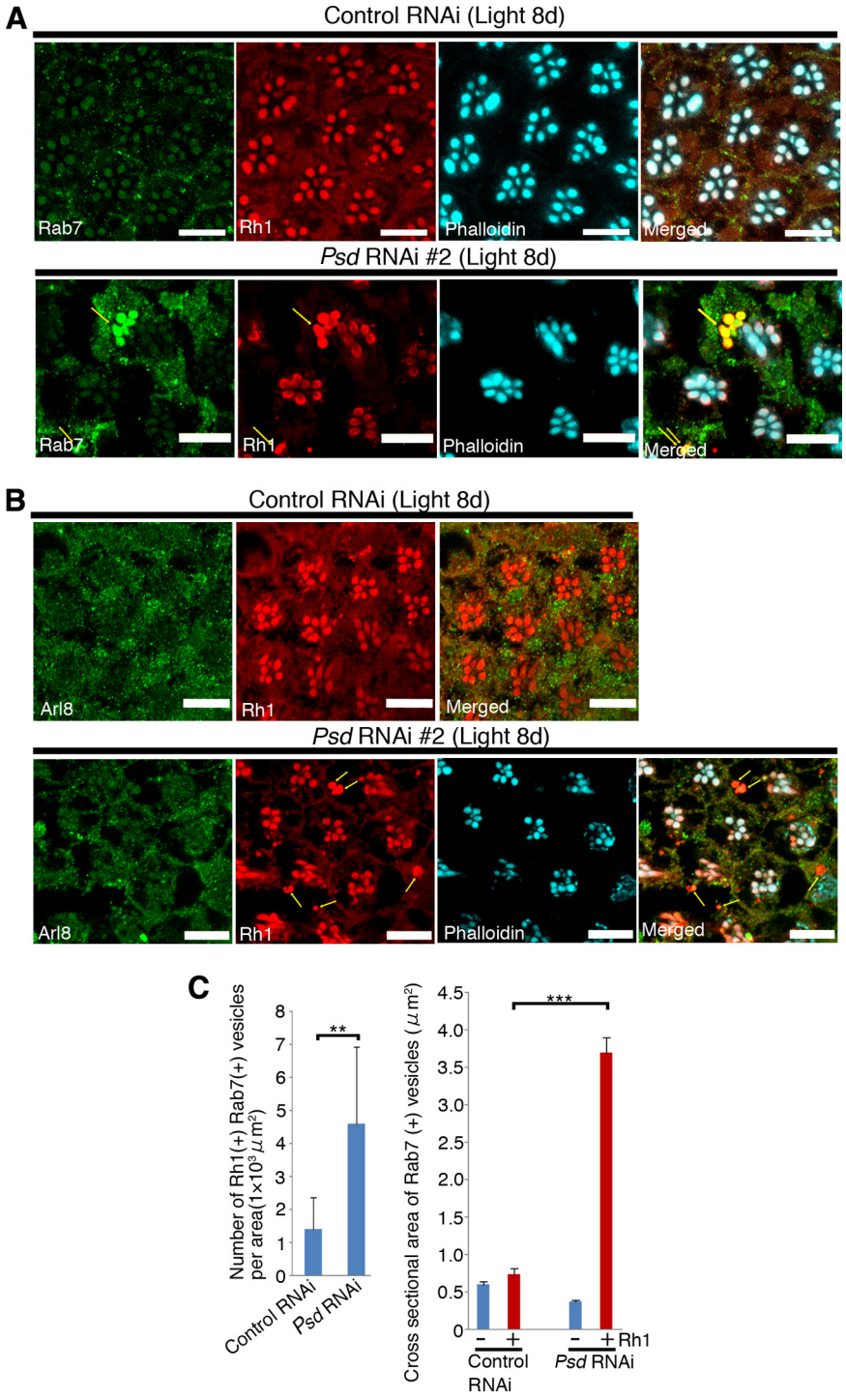

Figure 2. A *Psd* knockdown in *Drosophila* causes Rh1 accumulation in Rab7-positive endosomes in a light-dependent manner. ***A***, ***B***, Flies were reared under light exposure (8000 lux) for 8 d, and dissected retinas were stained as indicated in each panel. Rh1-positive large vesicles were found in the retinas of *Psd*-RNAi#2 flies (arrows) after light exposure. These vesicles colocalized with Rab7 (***A***, arrows) but not with Arl8 (***B***, arrows). Scale bars, 10 μm. ***C***, Statistical analysis of both Rh1- and Rab7-positive vesicles in the retinas of the *Psd* knockdown flies after light exposure for 8–10 d. Left, Number of both Rh1- and Rab7-positive vesicles per area was calculated from 10 to 14 images (4 to 7×10^3 μm^2/image) obtained from two to three independent experiments. The number of vesicles observed was significantly greater in *Psd*-RNAi flies compared with the control (*gfp*-RNAi). Values are the mean ± SD. $^{**}p < 0.01$, *t* test. Right, Cross sections of the Rh1-negative or Rh1-positive areas in Rab7-positive vesicles after light exposure for 8–10 d were measured. Both Rh1- and Rab7-positive vesicles observed in *Psd*-RNAi flies were significantly larger than those in the control (*gfp*-RNAi flies). Approximately 100 vesicles from two or three independent experiments were analyzed. Values are the mean ± SEM. $^{***}p < 0.001$, *t* test.

Urea–SDS-PAGE. Retinal cell extract was collected from 100 adult flies by excising the compound eyes followed by the removal of adherent brains and homogenization with lysis buffer. Then, 20 μg of retinal cell lysate was subjected to SDS-PAGE containing 6 M urea.

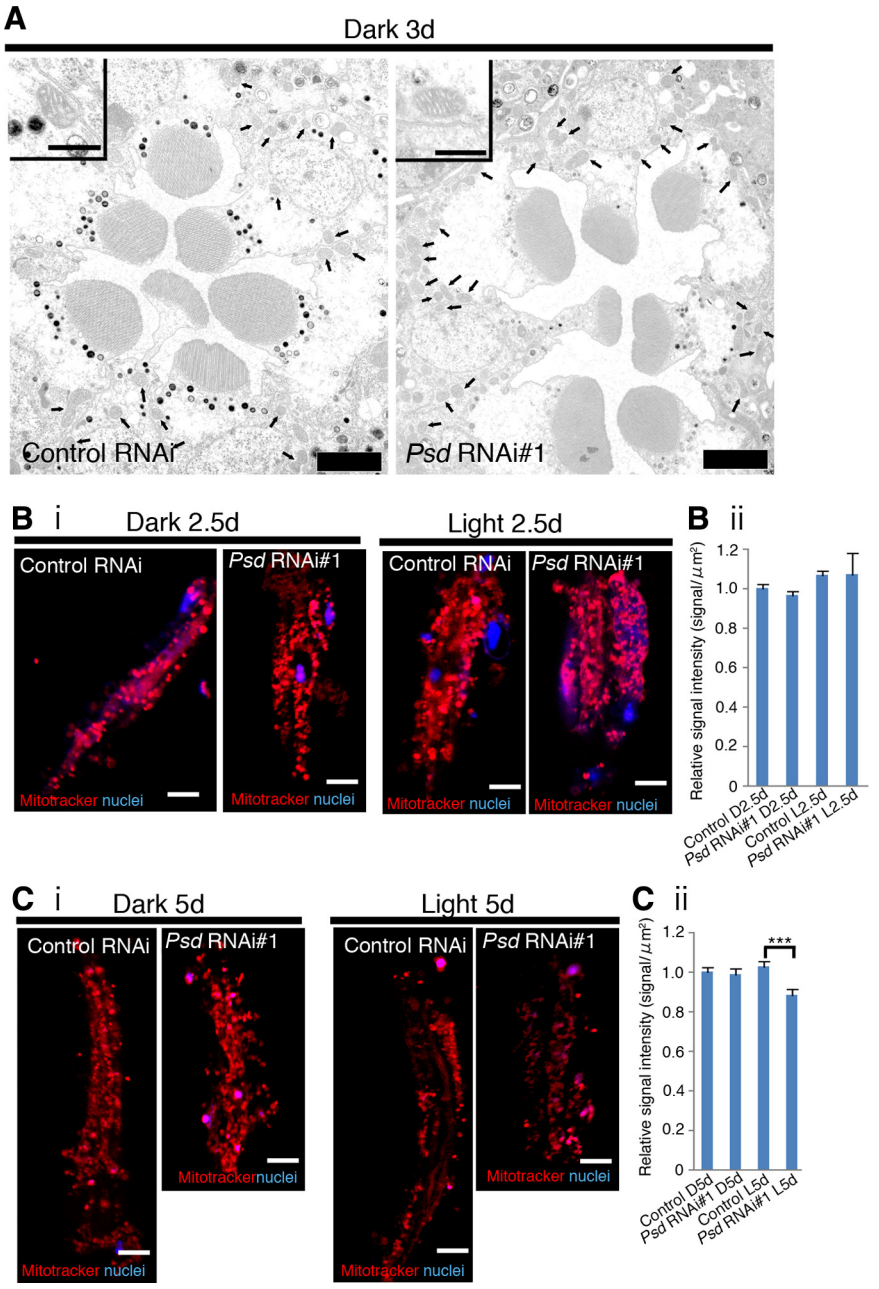

Figure 3. The *Psd* knockdown did not cause major mitochondrial dysfunction in retinal cells. ***A***, Transmission electron micrographs of *gfp*-RNAi and *Psd*-RNAi#1 retinas after dark rearing for 3 d. The morphology of the mitochondria (arrows) from both retina types did not show obvious differences. Scale bars, 2 μm. Mitochondria are highlighted in the insets. Scale bars, 0.5 μm. ***B***, ***C***, MitoTracker Red CMXRos labeling of cultured ommatidia collected from *gfp*-RNAi and *Psd*-RNAi#1 flies. Nuclei were labeled with TOPRO3. ***Bi***, Ommatidia collected from flies reared in the dark or exposed to light for 2.5 d. ***Bii***, Statistical analysis. Signal intensity of MitoTracker Red CMXRos-positive vesicles were measured from 10 to 15 ommatidia. Ten to 15 MitoTracker Red CMXRos-positive vesicles were measured meticulously from the end to the central region of each ommatidium ($n = 150$). The values shown are the mean ± SEM. ***Ci***, Ommatidia collected from flies reared in the dark or exposed to light for 5 d. ***Cii***, Statistical analysis. Signal intensities of MitoTracker Red CMXRos-positive vesicles were measured as shown in ***Bii***. MitoTracker signals in *Psd*-RNAi#1 flies did not decrease after dark rearing for 5 d, but showed a slight decrease after light exposure for 5 d compared with *gfp*-RNAi flies. The values shown are the mean ± SEM. ***$p < 0.001$, *t* test. Scale bars: ***Bi***, ***Ci***, 5 μm.

Retinoid-free medium. Retinoid-free medium (Sang's Medium) was prepared according to a protocol developed by Dr. William S. Stark (Saint Louis University, St. Louis, MO; http://starklab.slu.edu/Erg/tutorial.htm). To generate retinoid-deprived flies, the flies were reared from egg to adult on retinoid-free medium.

Terminal deoxynucleotidyl transferase-mediated biotinylated UTP nick end labeling assay. Adult fly heads were obtained and cut from the occipital foramen to the dorsal edge of the head, and fixed in 4% PFA, 0.1% Triton X-100 in PBS. The heads were then immersed in 12% sucrose, 0.1% Triton X-100 in PBS at 4°C for 8 h, and embedded in OCT compound. Frozen sections (20 μm thick) were prepared using a cryostat as described above and the terminal deoxynucleotidyl transferase-mediated biotinylated UTP nick end labeling (TUNEL) assay was performed using an Apo-BrdU *In Situ* DNA Fragmentation Assay kit (BioVision) according to the manufacturer's instructions.

Light exposure experiments. Flies were reared from the egg to third larval stage at 25°C under normal light exposure conditions and then reared until adulthood at 25°C in the dark. Hatched flies were then exposed to room light (4000 lux at 26–26.5°C or 8000 lux at 27–27.5°C) for 1–15 d as noted in each experiment. Flies reared in the dark at 26–26.5°C or at 27–27.5°C were prepared synchronously as controls (dark-reared flies) for the analysis of light-exposed flies.

Statistics. All statistical analyses were performed using the Microsoft Excel 2004 analysis toolpack. Significant differences among sample means were determined using Welch's *t* test.

Results

Knockdown of *Psd* in the *Drosophila* eye results in light-dependent retinal degeneration

To search for novel genes involved in retinal degeneration, we screened a library of RNA interference (RNAi)-inducible *Drosophila* strains by examining the formation of photoreceptor cells. The RNAi-inducible inverted repeat (IR) strains in this library harbor inverted repeats of *Drosophila* genes downstream of yeast upstream activating sequences (UASs) that are activated by the yeast Gal4 transcription factor (Nishihara et al., 2004). Crossing these IR strains with the eye-specific Gal4 driver strain (GMR-Gal4) leads to the eye-specific knockdown of the corresponding gene. In our present screen, sectioned eyes of the knockdown flies were stained with anti-Rh1, anti-Chp, or with phalloidin, which detects the presence of actin fibers in the rhabdomere. From this analysis, we found that knockdown of the *Drosophila Psd* gene (CG5991) resulted in the intracellular accumulation of Rh1 and the progressive destruction of photoreceptor cells under normal light conditions (Fig. 1*A*).

Retinal degeneration processes can be classified according to their light dependency. Defects in photoreceptor development or in rhodopsin folding/transport cause light-independent degeneration, whereas excessive rhodopsin internalization, the intracellular accumulation of rhodopsin, or the dysregulation of Ca^{2+} levels in photoreceptor cells cause light-dependent degradation (Alloway et al., 2000; Kiselev et al., 2000; Raghu et al., 2000; Webel et al., 2000; Orem and Dolph, 2002a; Orem et al., 2006). In this study, the

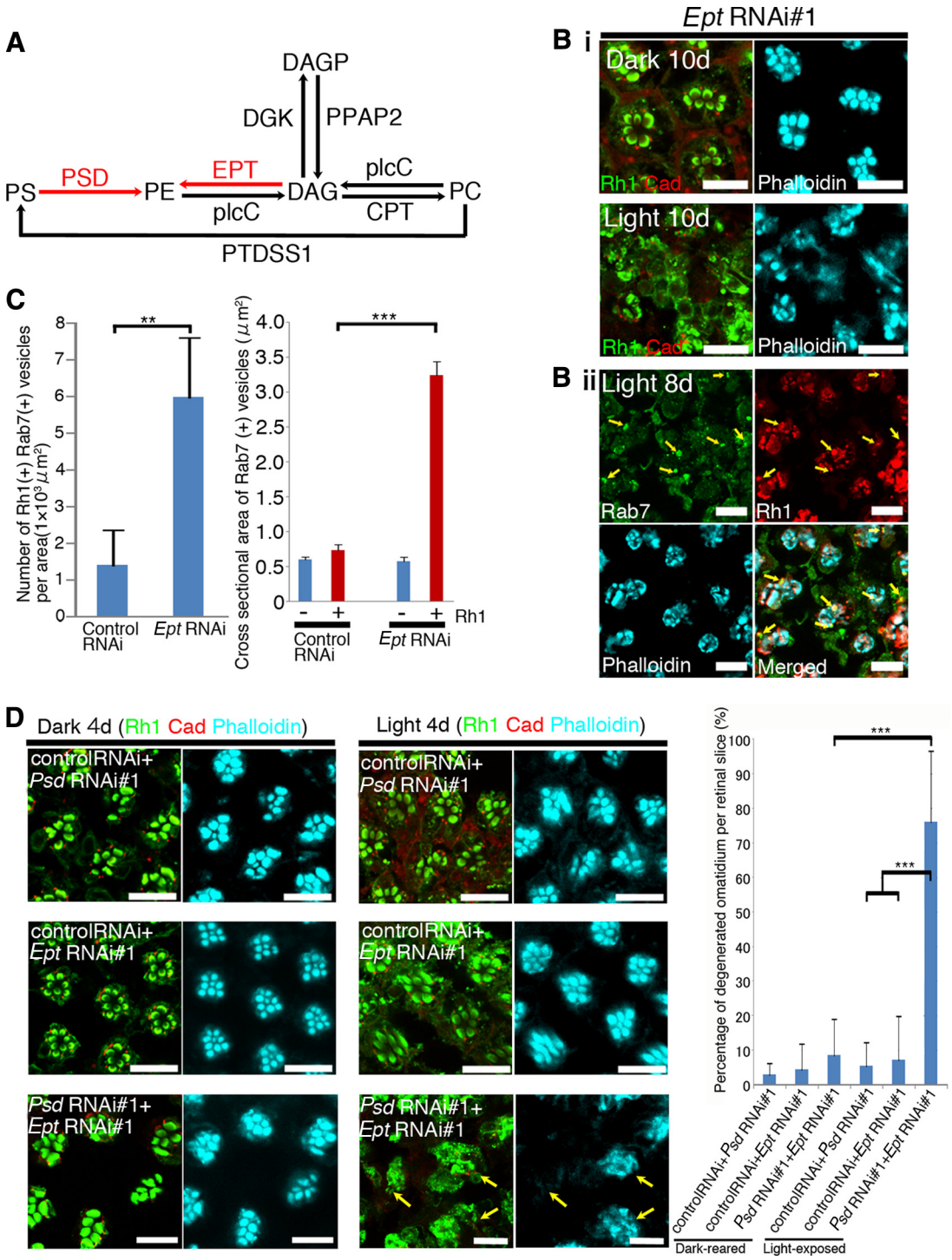

Figure 4. The suppression of PE synthesis causes light-dependent retinal degeneration. ***A***, Schematic representation of the *Drosophila* PE synthetic pathway according to the KEGG database (Kanehisa et al., 2008). ***Bi***, ***Bii***, An *Ept* knockdown also causes light-dependent retinal degeneration. Flies were reared, and dissected retinas were triply stained as indicated in each panel. Severe disruption of the ommatidia (***Bi***, arrows) was evident after light exposure for 10 d. Rh1-positive large vesicles were detected and observed to colocalize with Rab7 (***Bii***, arrows) after light exposure for 8 d. Scale bars, 10 μm. ***C***, Statistical analysis of both Rh1- and Rab7-positive vesicles in the retinas of *Ept* knockdown flies after light exposure for 8–10 d. Each value was calculated as shown in Figure 2*C*. Left, Number of both Rh1- and Rab7-positive vesicles per area. Values are the mean ± SD. $^{**}p < 0.01$, *t* test. Right, Cross section of an area of Rab7-positive vesicles. Values are the mean ± SEM. $^{***}p < 0.001$, *t* test. ***D***, The double knockdown of *Psd* and *Ept* enhances light-dependent retinal degeneration. Flies were reared and dissected retinas were triply stained as indicated at the top of the panels. Disrupted ommatidia (arrows) were evident in *Psd*-RNAi#1/*Ept*-RNAi#1 retinas. Scale bars, 10 μm. Right panel, Statistical analysis of retinal degeneration. Dissected retinal slices from eight flies were labeled as shown in the left panels, and the percentage of disrupted ommatidia per slice was calculated. More than nine slices obtained from two independent experiments were analyzed. The values shown are the mean ± SD. $^{***}p < 0.001$, *t* test.

knockdown of the *Psd* gene resulted in the loss of photoreceptor cells under light-exposed conditions, but showed only very marginal defects in dark-reared conditions (Fig. 1*B*). This suggested that the Psd protein is required for the normal processing of rhodopsin after its activation.

This light-dependent degeneration of the *Drosophila* retina allowed us to ascertain the primary defects in the *Psd* knockdown cells. To this end, sectioned eyes were stained with an anti-Rh1 antibody, or with phalloidin, to analyze the time-dependent degradation processes that occur after light exposure. Larvae and

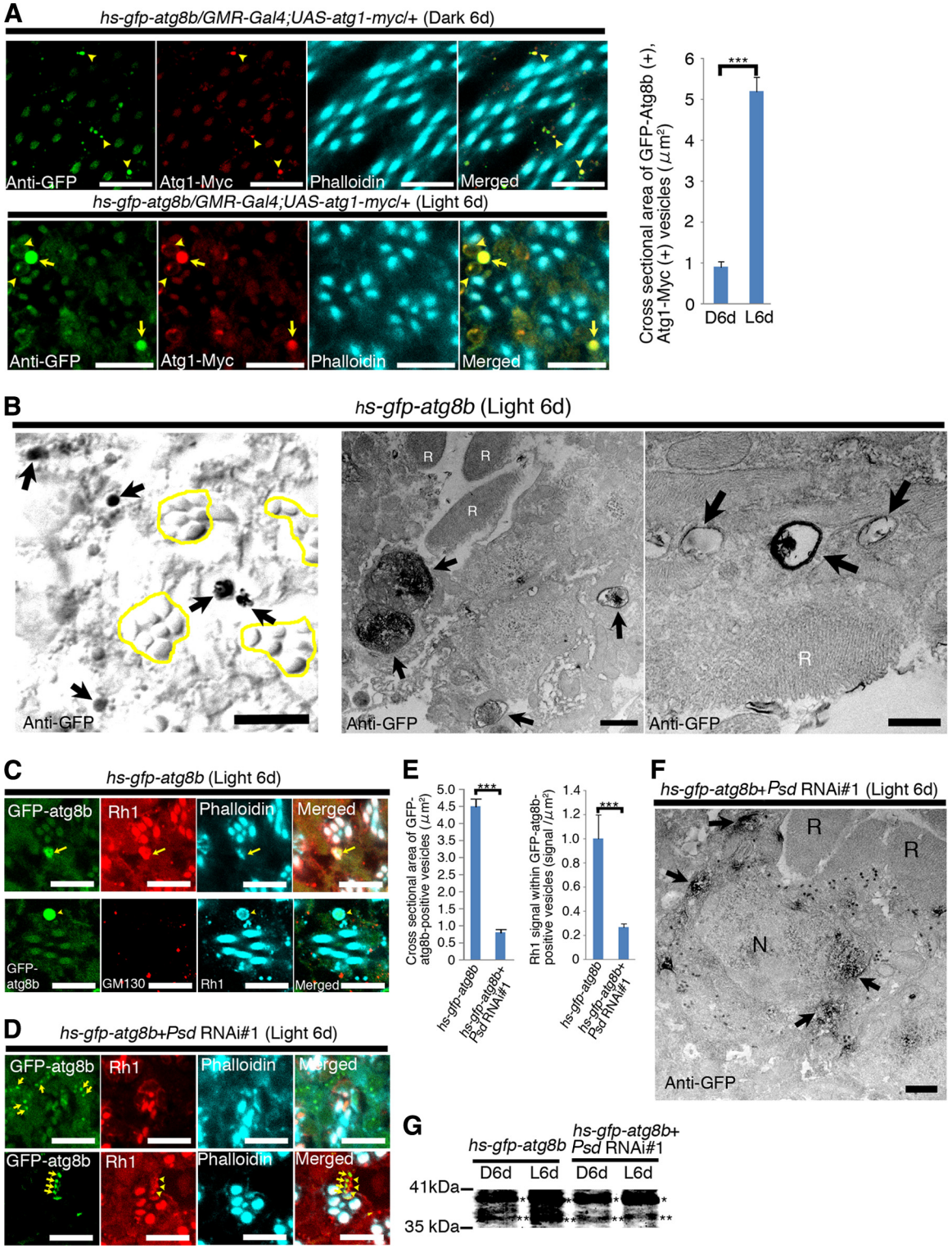

Figure 5. Autophagosome formation is dependent on *Psd*. ***A***, Left, Retinas of *hs-gfp-atg8b/GMR-Gal4; UAS-atg1-myc/+* flies stained with anti-GFP, anti-Myc, and phalloidin. Flies were incubated at 37°C for 50 min and reared in the dark or exposed to light for 6 d. The incubation at 37°C was repeated twice every 3 d. Whereas structures positive for GFP-Atg8b and Atg1-Myc were small (arrowheads in top panels) under dark conditions, they became larger after light exposure. Two types were detected: large punctate structures (arrows in bottom panels) and ring-shaped structures (arrowheads in bottom panels). Right, Cross-sectional area of GFP-atg8b and Atg1-Myc-positive vesicles ($n = 100$, 2 independent experiments). Values represent the mean ± SEM. $^{***}p < 0.001$, *t* test. Scale bars, 10 μm. ***B***, Immunodetection of GFP-Atg8b-positive structures by conventional (left) or electron (center, right) microscopy. Large structures (arrows in left panel) are revealed as vesicles containing residual membrane structures in their lumina (arrows in center and right panels), some of which are double-membrane vesicles. Rhabdomeres are indicated by yellow circles (left) or the letter "R" (center, right). Scale bars: left, 10 μm; center, right, 1 μm. ***C***, Double staining of retinas of control (*hs-gfp-atg8b*) flies after heat shock followed by light exposure (8000 lux) for 6 d. GFP-atg8b-positive autophagosomes/autolysosomes (arrows and arrowheads) were costained with anti-Rh1 and phalloidin (top panels, arrows), but not with anti-GM130 (bottom panels). ***D***, Double staining of retinas of *Psd* knockdown (*hs-gfp-atg8b*+*Psd*-RNAi#1) flies treated as shown in ***C***. The GFP-atg8b-positive vesicles (arrows) were smaller than those observed in control flies (shown in ***C***) and did not include Rh1 (arrowheads) or phalloidin. Scale bars: ***C***, ***D***, 10 μm. ***E***, Statistical analysis of GFP-atg8b-positive vesicles shown in ***C*** and ***D***. Left, Cross-sectional area containing GFP-atg8b-positive vesicles ($n = 80–100$, 2 independent experiments). Right, Rh1 signal within the range of GFP-Atg8b-positive vesicles ($n = 80–100$, 2 (*Figure legend continues.*)

pupae were grown in the dark and the hatched flies were exposed to light for a specific period. The *Psd* knockdown flies, reared in the dark for 5 d, showed normal rhabdomeres and no intracellular accumulation of Rh1 (Fig. 1*B*). The same normal phenotype was also observed in control photoreceptor cells in which GFP dsRNA had been induced (Fig. 1*B*). In contrast, *Psd* knockdown flies exposed to light for 2.5 d, showed an accumulation of Rh1 in comparatively large dotlike structures within the photoreceptor cells, but showed only marginal defects in the rhabdomeres (Fig. 1*B*). However, light exposure for 5 d caused severe defects in the rhabdomeres of these flies (Fig. 1*B*), and these defects were associated with apoptotic cell death as revealed by positive TUNEL staining (Fig. 1*C*). Hereafter, this rhabdomere defect was used as a histological marker of retinal degeneration in *Drosophila*. Collectively, these data clearly indicated that the intracellular accumulation of Rh1 was the primary defect in *Psd* knockdown flies.

To identify the compartment in which Rh1 accumulates after the knockdown of *Psd*, sectioned eyes were costained with several markers for these bodies. In the knockdown photoreceptor cells, accumulated Rh1 colocalized with Rab7, a late endosomal marker (Fig. 2*A*,*C*), but not with Avl8, a lysosomal marker (Fig. 2*B*), indicating that Rh1 accumulates in late endosomes in *Psd* knockdown retinas in a light-dependent manner.

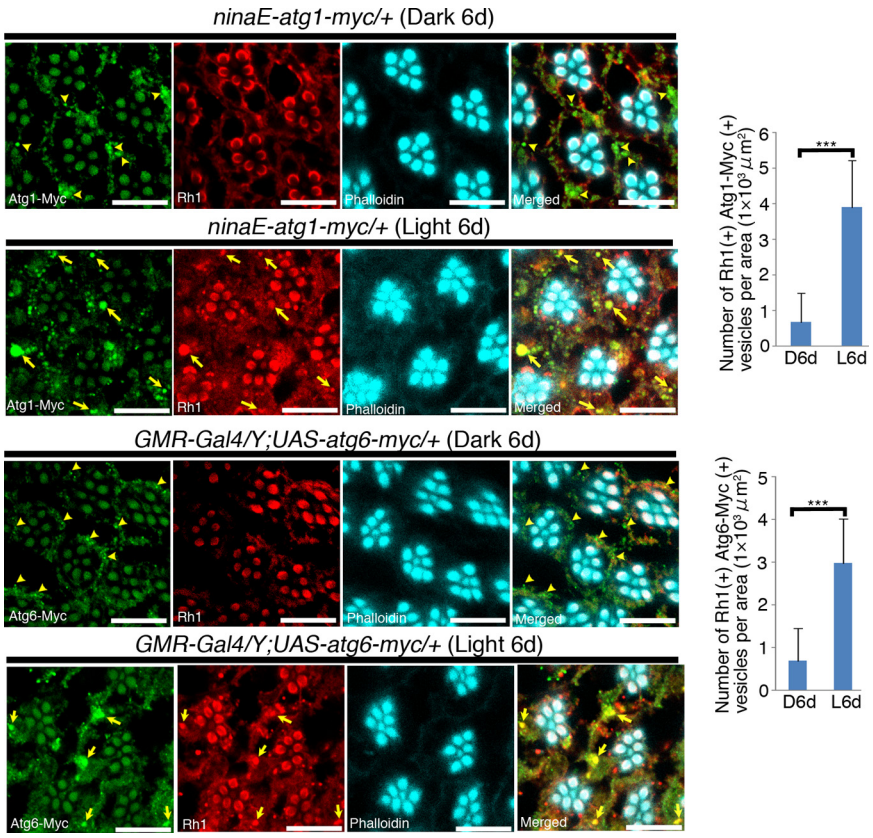

Figure 6. Light-dependent accumulation of Rh1 in Atg1- and Atg6-positive autophagosomes/autolysosomes. Left panels, Atg1-Myc- or Atg6-Myc-expressing flies were reared in the dark or under light exposure (8000 lux) for 6 d, and dissected retinas were triply stained as indicated in each panel. In retinas of dark-reared flies, both Atg1-Myc and Atg6-Myc were localized to the small punctate structures (arrowheads). In retinas of light-exposed flies, both Atg1-Myc and Atg6-Myc colocalized with Rh1 in large vesicles (arrows). Right, Statistical analysis of Atg1 and Rh1-positive (top) or Atg6 and Rh1-positive (bottom) vesicles shown in left panels. Each value was calculated as shown in Figure 2*C*. The number of both Atg1/Atg6 and Rh1-positive vesicles was significantly increased in light-exposed flies. Values are the mean ± SD. ***$p < 0.001$, *t* test. Scale bars, 10 μm.

The possibility that the observed retinal defects were attributable to an off-target effect of dsRNA was excluded by two experiments. In the first of these, a knockdown using a second set of dsRNAs corresponding to a different region of *Psd* was also found to cause the intracellular accumulation of Rh1 and late-onset retinal degradation (supplemental Fig. S1, available at www.jneurosci.org as supplemental material). There were neither overlapping, nor homologous sequences between the first and second sets of dsRNAs (see Materials and Methods). In the second experiment, coexpression of wild-type *Psd* with the targeting dsRNAs resulted in the partial rescue of retinal degeneration (supplemental Fig. S2, available at www.jneurosci.org as supplemental material). In addition, the levels of mRNAs for the targeted genes in the *Psd* knockdown eyes decreased compared with the wild-type levels (supplemental Fig. S3, available at www.jneurosci.org as supplemental material). The knockdown efficiencies of the dsRNAs used in this study were also examined and found to be sufficiently high in all cases.

The *Psd* knockdown did not cause severe mitochondrial dysfunction in retinal cells

The mouse *Psd* mutant exhibits deformed mitochondria (Steenbergen et al., 2005). Given that mitochondrial dysfunction can cause neural degeneration in mammals (Schapira, 2008), it is possible that the knockdown of *Psd* in *Drosophila* eyes may also induce retinal degeneration through mitochondrial dysfunction. To examine this possibility, we studied the morphology and function of the mitochondria in *Psd* knockdown cells. Morphological studies using electron microscopy revealed that the shapes and numbers of mitochondria were indistinguishable between the control and knockdown cells (Fig. 3*A*). In addition, mitochondrial function was also examined by comparing the uptake of the dye, MitiTrackerRed CMXRos, in control and knockdown cells. The uptake of this dye, whose accumulation depends on mitochondrial membrane potential (Brown et al., 2006), was indistinguishable between control and *Psd* knockdown photoreceptor cells that were exposed to light for 2.5 d (Fig. 3*B*) and showed light-induced accumulation of Rh1 (Fig. 1*B*). These data suggested that mitochondrial dysfunction is not related to Rh1 accumulation and retinal degeneration in *Psd* knockdown cells. However, light exposure for 5 d resulted in severe retinal degen-

←

(*Figure legend continued.*) independent experiments). Values are the mean ± SEM. ***$p < 0.001$, *t* test. ***F***, Immunodetection of GFP-Atg8b in *Psd* knockdown retinas. Anti-GFP signals were dispersed in some cytoplasmic domains (arrows). ***G***, PE conjugation of GFP-Atg8b in control (*hs-gfp-atg8b*) and *Psd* knockdown (*hs-gfp-atg8b*+*Psd*-RNAi#1) retinas. Flies were heat shocked and reared as indicated in ***A*** and then retinal cell extracts were subjected to urea–SDS-PAGE followed by immunoblotting using anti-GFP antibodies. The amount of PE-conjugated GFP-Atg8b was increased in control flies by light exposure, and this increase was suppressed by *Psd* knockdown. *GFP-Atg8b; **GFP-Atg8b-PE. Scale bars, 1 μm.

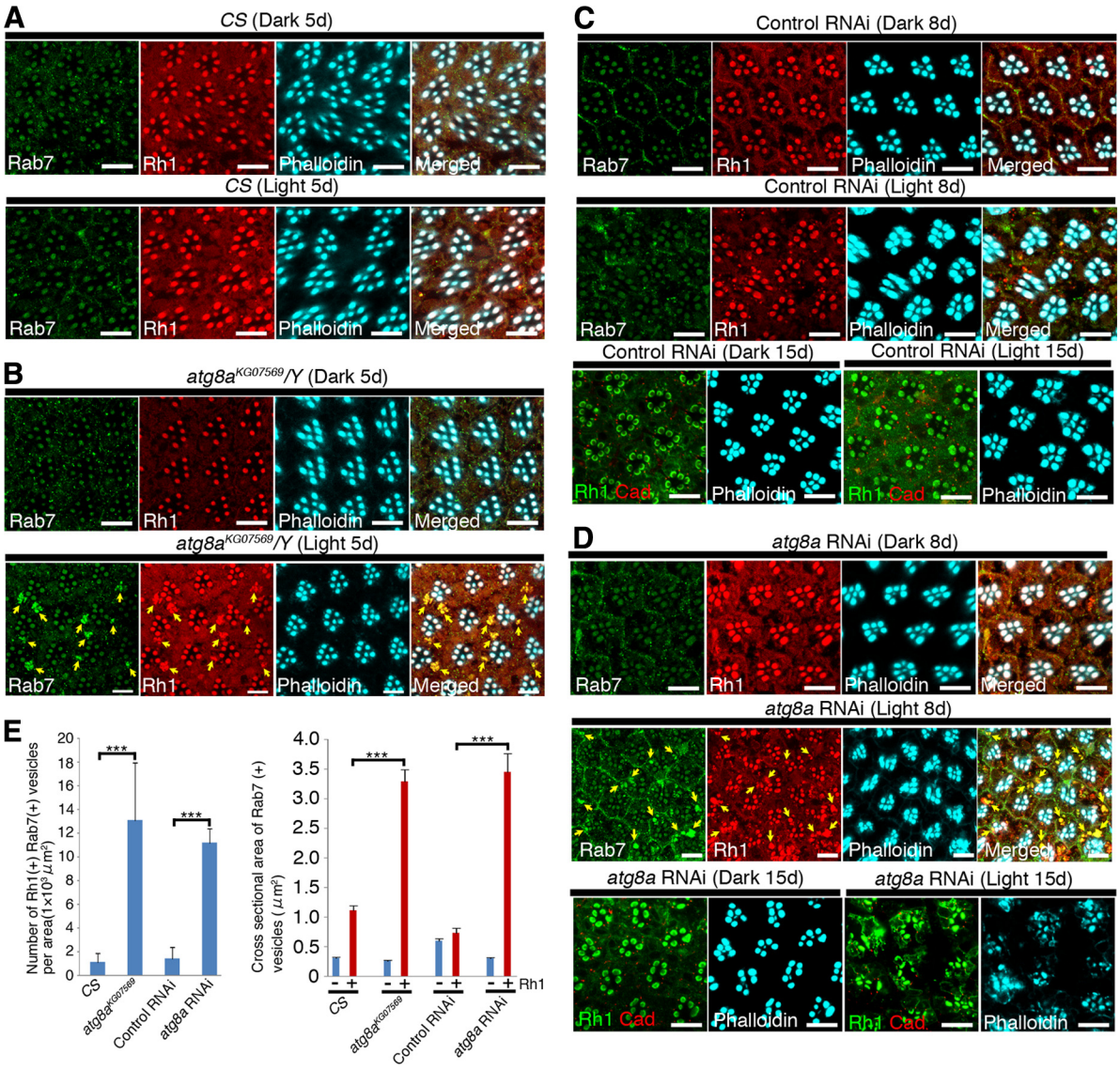

Figure 7. The suppression of *atg8a* causes Rh1 accumulation in Rab7-positive endosomes. ***A–D***, Immunostaining of dissected retinas. The flies were treated and dissected retinas were triply stained as indicated in each panel. ***A***, CS (Canton-S, wild-type) flies. ***B***, *atg8a*^{KG07569} flies. Rh1 accumulation was found in Rab7-positive endosomes (arrows) after light exposure. ***C***, *gfp*-RNAi flies. ***D***, *atg8a*-RNAi flies. After light exposure for 8 d, Rh1-positive large vesicles were found in all of the ommatidia and colocalized with Rab7 (arrows). After light exposure for 15 d, the reduction or loss of rhabdomeres (arrowheads) was found throughout the range of ommatidia. Scale bars: ***A–D***, 10 μm. ***E***, Statistical analysis of Rh1- and Rab7-positive vesicles after light exposure (5 d for CS and *atg8a*^{KG07569} flies, and 8 –10 d for *gfp*-RNAi and *atg8a*-RNAi flies). Left, Number of Rh1- and Rab7-positive vesicles per area was calculated as shown in Figure 2*C*. Values are the mean ± SD. ***$p <$ 0.001, *t* test. Right, Cross section of the area containing Rab7-positive vesicles observed after light exposure was calculated as shown in Figure 2*C*. Values are the mean ± SEM. ***$p < 0.001$, *t* test.

eration (Fig. 1*B*) and a slight reduction in the uptake of the dye (Fig. 3*C*). This late-onset defect of mitochondria may be a secondary effect of retinal degeneration or other defects caused by *Psd* knockdown.

Ept knockdown also causes defective Rh1 transport and light-dependent retinal degradation

As shown above, Psd is required for the viability of photoreceptor cells in the *Drosophila* retina. Since Psd generates PE through the decarboxylation of phosphatidylserine (PS), we questioned whether a reduction in PE levels could be responsible for retinal degeneration. PE is synthesized in two major pathways, the PS decarboxylation pathway and the CDP-ethanolamine pathway (Fig. 4*A*). Ept catalyzes the final reaction step in the CDP-ethanolamine pathway in the ER. In this study, the knockdown of *Ept* caused Rh1 accumulation in Rab7-positive late endosomes and light-dependent retinal degeneration (Fig. 4*B*,*C*), as was also observed in the *Psd* knockdown eyes. The same phenotype was also caused by the knockdown of *Ept* using a dsRNA corresponding to a different region of the *Ept* gene (supplemental Fig. S4, available at www.jneurosci.org as supplemental material), excluding the possibility that off-target RNAi effects were responsible.

In addition, we found that a genetic interaction exists between *Psd* and *Ept*. A weak induction of dsRNAs for *Psd* or *Ept* produced almost normal photoreceptors (Fig. 4*D*); however, under the same conditions, the induction of dsRNAs for both *Psd* and *Ept* caused severe degeneration of photoreceptors after light exposure for 4 d. Furthermore, neither Rh1 accumulation, nor retinal degeneration was caused by the knockdown of diacylglycerol cholinephosphotransferase (*cpt*, CG7149) or CDP-diacylglycerol-serine *O*-phosphatidyltransferase (*ptdss1*, CG4825) (supplemental Fig. S5, available at www.jneurosci.org as supplemental material), which are essential for the production of PC (phosphatidylcholine) and PS, respectively (Fig. 4*A*). Together,

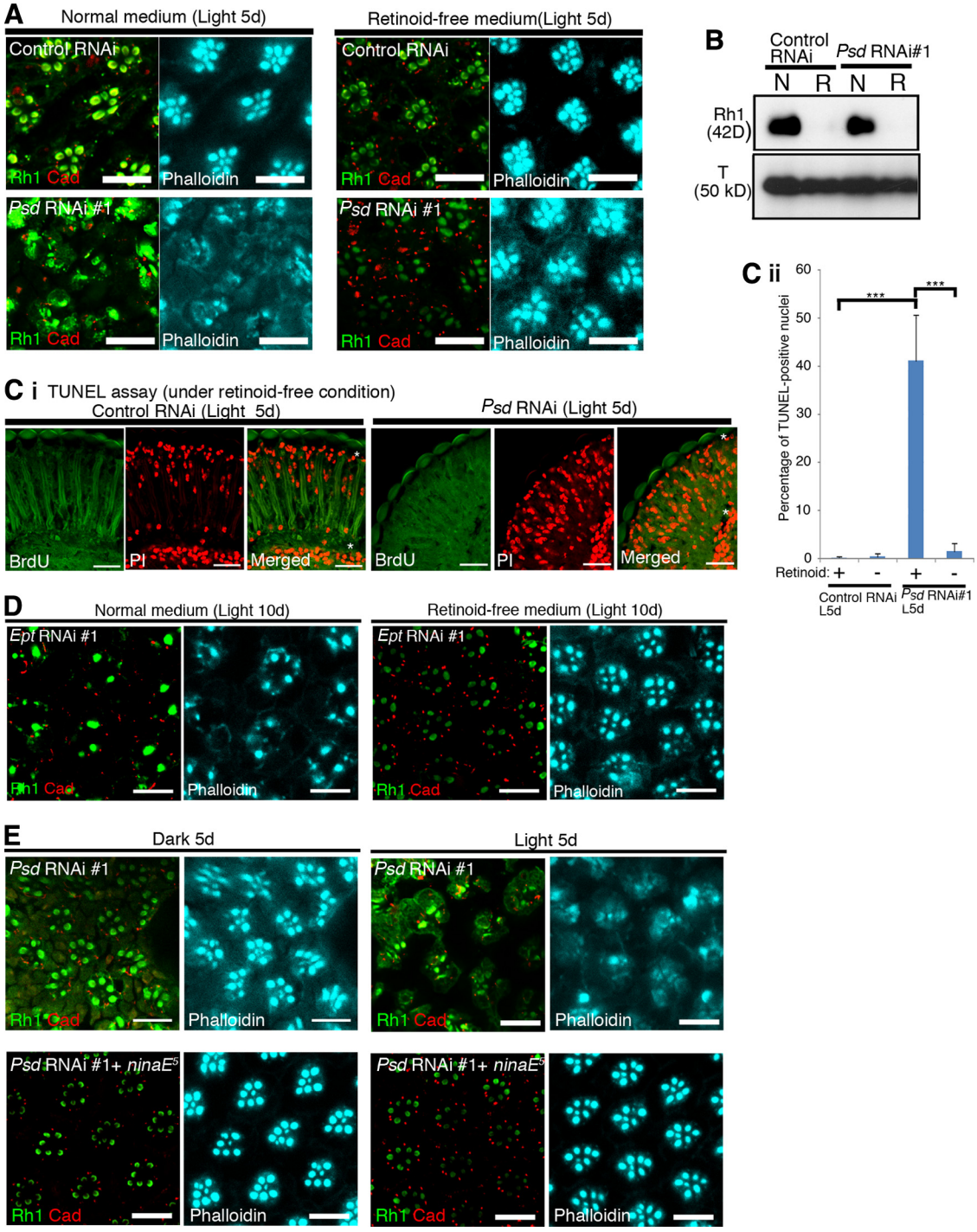

Figure 8. The suppression of Rh1 synthesis rescues light-dependent retinal degeneration in *Psd*-RNAi flies. ***A***, Triple staining of dissected retinas from *gfp*-RNAi and *Psd*-RNAi#1 flies. Flies were reared on either normal medium (left panels) or retinoid-free medium (right panels) for 5 d under light exposure (4000 lux). *Psd*-RNAi flies, deprived of retinoids, showed resistance to light-dependent retinal degeneration. Scale bars, 10 μm. ***B***, Immunoblotting of adult head lysates collected from *gfp*-RNAi and *Psd*-RNAi#1 flies reared on normal medium (N) or retinoid-free medium (R) in the dark. Lysate from one-half of the harvested adult heads was immunoblotted with anti-Rh1 (Rh1) (top panel) or anti-α-tubulin (T) (bottom panel) antibodies. ***C***, Retinoid deprivation suppresses the light-dependent retinal cell death of *Psd*-RNAi#1 flies. ***Ci***, *gfp*-RNAi and *Psd*-RNAi#1 flies were reared on normal medium (as shown in Fig. 1*Ci*) or retinoid-free medium (this figure) under light exposure at 4000 lux for 5 d. A TUNEL assay was then performed as described in Figure 1*C*. The retinal cell death observed in light-exposed *Psd*-RNAi#1 flies was completely suppressed by retinoid deprivation. Scale bars, 20 μm. ***Cii***, Statistical analysis of TUNEL-positive nuclei. The percentage of TUNEL-positive nuclei located from the apical surface to the retinal floor (shown by asterisks in the merged images in ***Ci***) was calculated as in Figure 1*Cii*. The values are the mean $\pm$ SD. $^{***}p < 0.001$, *t* test. ***D***, Triple staining of the dissected retinas of *Ept*-RNAi#1 flies reared on either normal medium (left panels) or retinoid-free medium (right panels) for 10 d under light exposure (8000 lux). The *Ept*-RNAi flies, deprived of retinoid, showed resistance to light-dependent retinal degeneration. Scale bars, 10 μm. ***E***, The light-dependent retinal degeneration observed in *Psd* knockdown flies was rescued by an *rh1* mutation, *ninaE*. *Psd*-RNAi#1 or *Psd*-RNAi#1 + *ninaE5* flies were reared and triply stained as indicated in each panel. The severe impairment of ommatidia caused by the *Psd* knockdown after light exposure was completely suppressed by the *rh1* mutation. Scale bars, 10 μm.

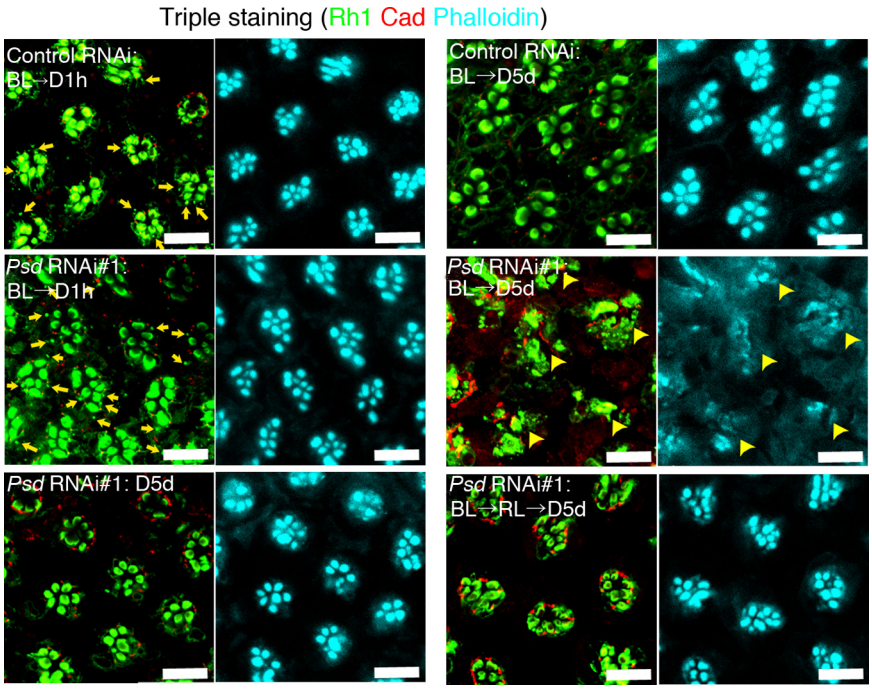

Figure 9. Blue/red light exposure reversibly induces retinal degeneration in *Psd* knockdown flies. The *gfp*-RNAi and *Psd*-RNAi#1 flies were treated as indicated in each panel and dissected retinas were triply stained (Rh1, Cad, and phalloidin). Rh1-positive puncta, possibly originating from internalized Rh1, were found in both types of flies (arrows) after blue light exposure (22,000 lux) for 10 min followed by 1 h of darkness (BL→D1h). The ommatidia of *Psd*-RNAi#1 flies were severely impaired (arrowheads) after blue light exposure for 10 min followed by 5 d in the dark (BL→D5d). The retinal degeneration induced by blue light exposure was suppressed by subsequent red light exposure (4000 lux) for 10 min (BL→RL→D5d). Scale bars, 10 μm.

these results demonstrated that retinal degeneration caused by *Psd* or *Ept* knockdown was attributable to a reduction in PE.

Autophagosomes containing Rh1 are deformed by *Psd* knockdown

Since PE is an essential component of autophagosomes, autophagosome formation was examined in *Psd* knockdown photoreceptor cells. To detect autophagosomes *in situ*, we expressed the following autophagosomal/autolysosomal markers in photoreceptor cells: GFP-conjugated Atg8b (GFP-Atg8b), Myc-tagged Atg1 (Atg1-Myc), and Myc-tagged Atg6 (Atg6-Myc) (Scott et al., 2004; Tekinay et al., 2006; Sun et al., 2008; Venkatachalam et al., 2008). Whereas only small punctate areas, positive for both GFP-Atg8b and Atg1-Myc, were detected under dark-reared conditions, these double-positive structures were much larger after exposure to light (Fig. 5*A*). Immuno-electron-microscopic analysis, using an anti-GFP antibody, revealed that these larger structures, which were also positive for Atg6-Myc (Fig. 6), were vesicles containing residual membranous structures in their lumina (Fig. 5*B*, arrows), some of which were double-membrane vesicles. This EM data strongly suggested that these structures were autophagosomes/autolysosomes. In addition, we found that, under light-exposed conditions, these autophagosomes/autolysosomes were positive for Rh1 (Figs. 5*C*, 6), but not for the Golgi marker, GM130 (Fig. 5*C*).

The large autophagosomes/autolysosomes were not formed in *Psd* knockdown cells and only small structures remained that contained little Rh1 (Fig. 5*D*,*E*). Consistently, immuno-electron-microscopic studies confirmed that the double-membrane vesicles were rarely detected in the *Psd* knockdown cells and revealed cytoplasmic domains stained by anti-GFP antibody (Fig. 5*F*, arrows). These anti-GFP-positive domains may correspond to the small punctate signals in Figure 5*D* (arrows). This reduction in autophagosome size and number was consistent with previous reports, which showed that the number and size of autophagosomes were also reduced in *Drosophila atg7* and *atg3* mutants (Juhász et al., 2003, 2007).

Next, we investigated the molecular basis for the deformation of autophagosomes in *Psd* knockdown cells. Given that the PE-conjugated form of Atg8 is essential for autophagosome formation in yeast and mammals, we analyzed the amount of Atg8-PE present in cells biochemically. Lysates from control and *Psd* knockdown retinas were subjected to urea–SDS-PAGE, since free Atg8 and PE-conjugated Atg8 migrate at different rates (Kirisako et al., 2000; Amar et al., 2006). Consistent with the light-induced formation of autophagosomes, levels of Atg8-PE were elevated by light exposure in the control retinas (Fig. 5*G*). This elevation was not observed in the knockdown cells (Fig. 5*G*), suggesting that Psd is required for autophagosome formation since it is involved in the synthesis of PE, the substrate of Atg8-PE.

An *atg8a* mutation or knockdown of *atg8a* or *atg7* causes Rh1 accumulation and retinal degeneration

Given that both autophagosome deformation and Rh1 accumulation result from *Psd* knockdown, we examined whether autophagy is required for the efficient degradation of Rh1. Since Atg8 and Atg7 are essential for autophagosome formation, we analyzed the following mutant and knockdown flies: *atg8a* mutant ($atg8a^{KG07596}$) and RNAi-inducible IR strains, *atg8a* and *atg7*. In $atg8a^{KG07596}$ mutant eyes, Rh1 accumulated in compartments that were Rab7-positive and phalloidin-negative (Fig. 7*B*,*E*); this was also observed in the *Psd* and *Ept* knockdown cells. The $atg8a^{KG07596}$ animals had very poor health and the escaped adults died before retinal degeneration occurred. Hence, we focused our analysis on the knockdown flies. We observed Rh1 accumulation and severe retinal degeneration in the Rab7-positive endosomes of the *atg8a* or *atg7* knockdown photoreceptor cells (Fig. 7*D*,*E*; supplemental Fig. S6, available at www.jneurosci.org as supplemental material). In addition, these phenotypes were not induced under dark-reared conditions (Fig. 7*B*,*D*; supplemental Fig. S6*A*, available at www.jneurosci.org as supplemental material). Together, we concluded from our data that autophagy is required for efficient Rh1 degradation under light exposure and that impaired autophagy results in retinal degeneration.

A reduction in rhodopsin expression rescued retinal degeneration caused by *Psd* knockdown

Given that impairment of the autophagic pathway resulted in the intracellular accumulation of Rh1 followed by retinal degeneration, we wanted to examine whether the main cause of this phenotype was the accumulation of excess Rh1. The expression of rhodopsins is reduced when *Drosophila* is grown in retinoid-free

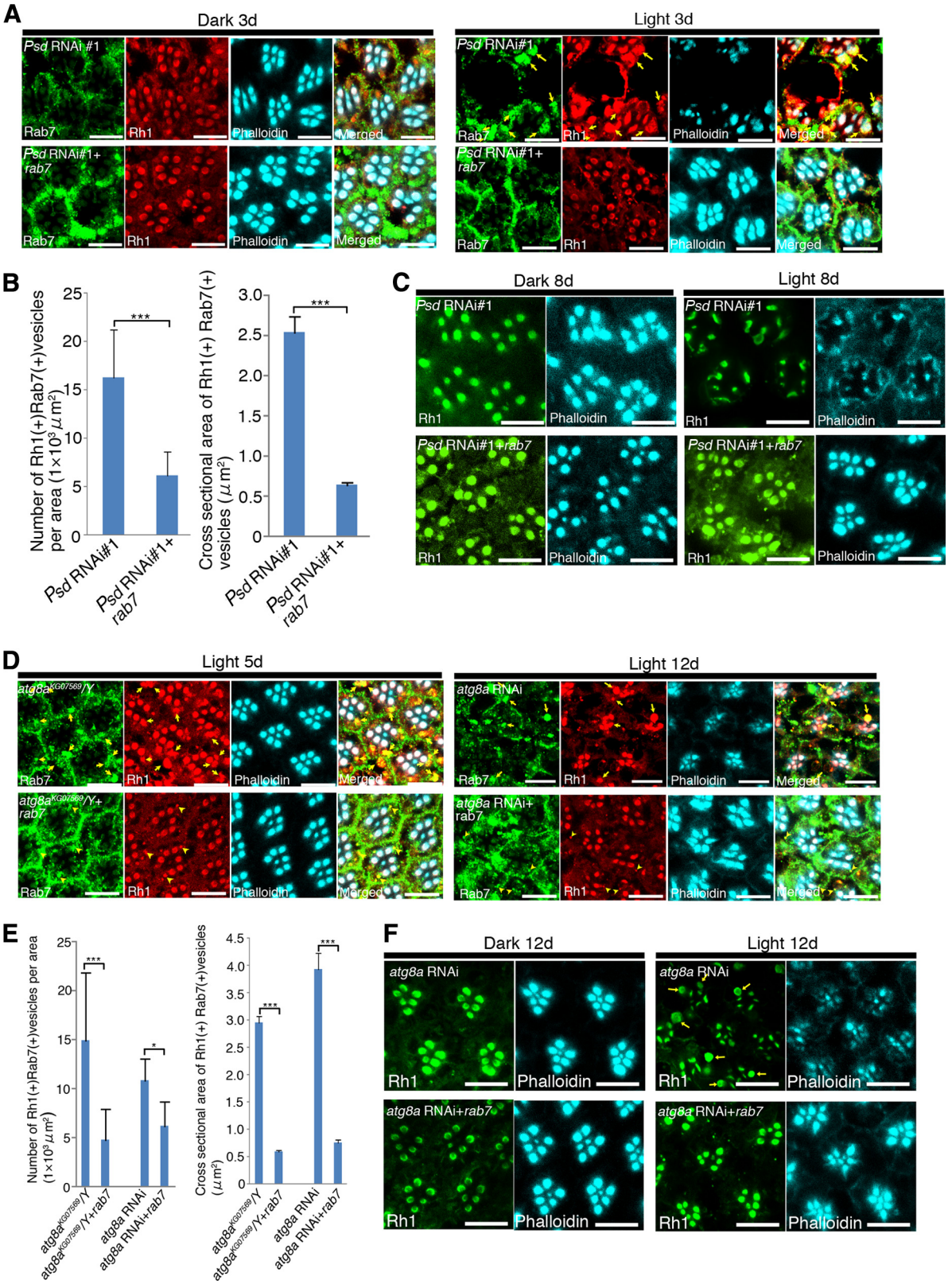

Figure 10. Overexpression of Rab7 suppresses light-dependent retinal degeneration in autophagy deficient flies. ***A***, Rab7 expression suppresses Rh1 accumulation in late endosomes caused by *Psd* knockdown. The *Psd*-RNAi#1 (top panels) flies and *Psd*-RNAi#1 flies carrying the *rab7* gene (bottom panels) were reared in the dark or exposed to light (8000 lux) for 3 d. The retinas were triply stained as shown in each panel. The number and size of large Rh1-positive late endosomes (arrows) shown in light-exposed *Psd*-RNAi#1 retinas were clearly reduced by Rab7 expression. ***B***, Statistical analysis of Rh1- and Rab7-positive vesicles after light exposure for 3 d. Left, Number of Rh1- and Rab7-positive vesicles per area was calculated as shown in Figure 2*C*. Values are the mean ± SD. ***$p < 0.001$, *t* test. Right, Cross-sectional area of Rh1- and Rab7-positive vesicles. Values are the mean ± SEM. ***$p < 0.001$, *t* test. ***C***, Rab7 expression suppresses light-dependent retinal degeneration in *Psd*-RNAi#1 retinas. Flies were reared in the dark or exposed to light (8000 lux) for 8 d, and the retinas were doubly stained as shown in each panel. Ommatidial deformation caused by *Psd* knockdown under light-exposed conditions was completely suppressed by Rab7 expression. ***D***, Rab7 expression suppresses Rh1 accumulation in late endosomes caused by the *atg8a* mutation (*atg8a*^{KG07569})/knockdown (*atg8*-RNAi). The *atg8a* mutant/knockdown flies (top panels) and *atg8a* mutant/knockdown flies bearing the *rab7* gene (bottom panels) were reared in the dark, or (*Figure legend continues.*)

medium (Fig. 8*A*,*B*) (Picking et al., 1996; Orem and Dolph, 2002b), and the *Psd* knockdown flies grown in retinoid-free medium showed neither intracellular accumulation of Rh1, nor retinal degeneration under light-exposed conditions, whereas flies cultured in normal medium showed severe retinal degeneration (Fig. 8*A*). In addition, TUNEL staining revealed that no cell death occurred in the *Psd* knockdown flies grown in retinoid-free medium (Fig. 8*C*). The retinal degeneration caused by the *Ept* knockdown was also suppressed under retinoid-free conditions (Fig. 8*D*).

The expression of Rh1 was also reduced by introduction of the *rh1* mutant allele, $ninaE^5$, which reduced the levels of Rh1 to between 3 and 13% of that of the wild type (flybase; http://flybase.org/reports/FBgn0002940.html). Light-dependent retinal degeneration in the *Psd* knockdown photoreceptor cells was also clearly suppressed by the introduction of the $ninaE^5$ mutation (Fig. 8*E*). These results suggested that PE reduction induces retinal degeneration through the excess accumulation of rhodopsin.

The results of another series of experiments supported this conclusion. Rh1 is inactivated by red light (~580 nm) (Kiselev et al., 2000), whereas treatment with blue light (~480 nm) followed by red light exposure causes transient activation but no internalization of Rh1. In our current analyses, we found that blue light exposure for 10 min followed by 1 h of darkness caused internalization of Rh1 in the *Psd* knockdown flies (Fig. 9). When such flies were reared in the dark for >5 d, the photoreceptors became severely deformed (Fig. 9). In contrast, blue light exposure followed by 10 min of red light exposure blocked Rh1 internalization and no retinal degradation occurred even after rearing in the dark for an additional 5 d (Fig. 9). These results further suggested that the internalization of Rh1 is responsible for the underlying retinal degeneration caused by the impairment of the autophagic pathway.

Overexpression of Rab7 rescues retinal degeneration caused by impairment of the autophagic pathway

The internalized Rh1 accumulated in the Rab7-positive endosomes because of the impairment of the autophagic pathway, suggesting cross talk between the autophagic and endosomal degradation pathways. To test this theory, we examined whether retinal degeneration caused by impaired autophagy was rescued by use of the endosomal degradation pathway. We overexpressed Rab7, which accelerates late endosome to lysosome trafficking of proteins requiring degradation (Entchev et al., 2000; Seto et al., 2002), in the *Psd* and *atg8a* knockdown photoreceptor cells. The overexpression of Rab7 caused a significant reduction in the accumulation of Rh1 (Fig. 10*A*,*B*) and rescued retinal degeneration in light-exposed *Psd* knockdown flies (Fig. 10*C*). We found consistently that the accumulation of excess Rh1 in Rab7-positive endosomes in the *atg8a* mutant and knockdown cells, and the light-dependent retinal degeneration seen in *atg8* knockdown flies, were also suppressed by Rab7 overexpression (Fig. 10*D*–*F*). These data suggested that the autophagic and endosomal pathways cooperatively degrade excess Rh1 that is internalized by light exposure.

The suppression of *Ppt1* causes retinal degeneration in *Drosophila* and this defect is enhanced synergistically by *Psd* knockdown

Since it is known that *Psd* interacts genetically with the *Drosophila* ortholog of human *PPT1*, a gene that is mutated in the pediatric neurodegenerative disease known as infantile neuronal ceroid lipofuscinosis (INCL) (Glaser et al., 2003; Hickey et al., 2006), we expected that palmitoyl-protein thioesterase 1 (Ppt1) in *Drosophila* would be essential for the viability of photoreceptor cells. Therefore, we analyzed the phenotype of the *Ppt1* knockdown. In *Ppt1* knockdown cells, light exposure induced Rh1 accumulation in the Rab7-positive late endosome, and this was followed by retinal degeneration (Fig. 11*A*; supplemental Fig. S7, available at www.jneurosci.org as supplemental material) associated with cell death (Fig. 11*B*). However, these events were suppressed when the knockdown flies were grown in retinoid-free medium (Fig. 11*A*–*C*), suggesting that Rh1 accumulation is the cause of the degeneration. In addition, light-dependent degeneration also occurred in the *Ppt1* mutants, *Df(1)446-20* and $Ppt1^{S77F}$ (supplemental Fig. S8, available at www.jneurosci.org as supplemental material), excluding the possibility that off-target effects of RNAi were responsible for the observed anomalies. Collectively, therefore, our data indicated that Ppt1 is essential for photoreceptor viability in *Drosophila*.

The genetic interaction between the *Psd* and *Ppt1* loss-of-function alleles was examined because a previous study described an interaction between overexpressed *Ppt1* and *Psd* (Buff et al., 2007). To test this, dsRNAs for *Psd* and *Ppt1* were induced simultaneously using weak conditions under which expression of each one of the dsRNAs did not cause severe defects (Fig. 11*D*). However, the simultaneous induction of both dsRNAs produced severe defects and a count of the degenerated ommatidia per retinal slice clearly revealed the synergistic enhancement of retinal degeneration (Fig. 11*D*). These results suggest that *Psd* and *Ppt1* undergo a genetic interaction under conditions of reduced expression.

Discussion

Degradation of rhodopsin by autophagy

In this *Drosophila* study, we have demonstrated that Rh1, a major rhodopsin, is degraded by autophagy, in addition to the endosomal degradation pathway, and that defects in the autophagic pathway cause light-dependent retinal degeneration. PE, a lipid found in the membrane of autophagosomes, is synthesized by Psd in mitochondria and by Ept in the ER and nuclear envelope (Choi et al., 2005; Vance, 2008). Using an eye-specific knockdown screen with an inducible RNAi library, we identified Psd as an essential factor involved in the prevention of light-dependent retinal degeneration in *Drosophila*. Psd-deficient mice die at around embryonic day 9, before neural cells differentiate (Steenbergen et al., 2005), and it is possible that this lethality might be attributable to mitochondrial defects, since fibroblasts established from Psd-deficient mice exhibit fragmented, aberrantly shaped mitochondria. Given that mitochondrial defects have been implicated in neurodegeneration, such defects might also contribute to the retinal degeneration observed in the *Psd* knock-

←

(*Figure legend continued.*) exposed to light (8000 lux) for 5 or 12 d, and the retinas were triply stained as shown in each panel. The number and size of large Rh1-positive late endosomes (arrows) shown in light-exposed *atg8a* mutant/knockdown retinas were reduced by Rab7 expression (arrowheads). ***E***, Statistical analysis of Rh1- and Rab7-positive vesicles after light exposure for 5 or 12 d. Each value was calculated as shown in ***B***. Values are the mean ± SD and the mean ± SEM in left and right graphs, respectively. $*p < 0.05$, $***p < 0.001$, *t* test. ***F***, Rab7 expression suppresses light-dependent retinal degeneration caused by *atg8a* knockdown. Flies were reared in the dark or exposed to light (8000 lux) for 12 d, and the retinas were doubly stained as shown in each panel. The retinal degeneration caused by *atg8a* knockdown after light exposure was suppressed by Rab7 expression. The arrows indicate Rh1-positive large vesicles. Scale bars: ***A***, ***C***, ***D***, ***F***, 10 μm.

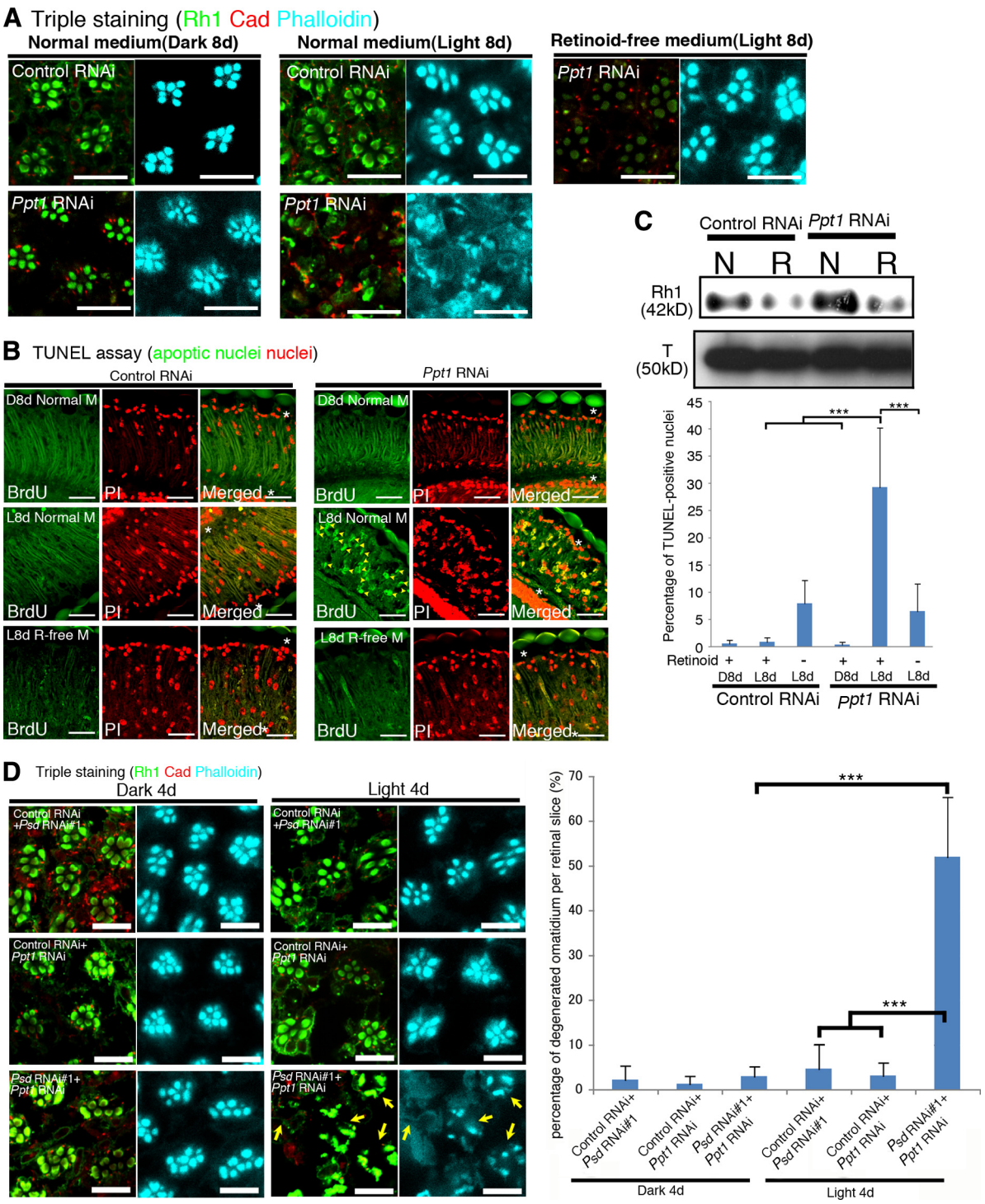

Figure 11. The *Ppt1* knockdown causes light-dependent retinal degeneration and genetically interacts with the *Psd* knockdown. ***A***, Triple staining of the dissected retinas of flies bearing two copies of *gfp*-RNAi (*gfp*-RNAi/*gfp*-RNAi) or *Ppt1*-RNAi (*Ppt1*-RNAi/*Ppt1*-RNAi). Flies were reared on either normal medium (left and middle panels) or retinoid-free medium (right panels) for 8 d under dark-reared (left panels) or light-exposed (8000 lux, middle and right panels) conditions. The *Ppt1*-RNAi/*Ppt1*-RNAi flies, deprived of retinoids, showed resistance to light-dependent retinal degeneration. Scale bars, 10 μm. ***B***, A TUNEL assay was then performed as described in Figure 1*Ci*. Light-dependent photoreceptor cell death in *Ppt1*-RNAi/*Ppt1*-RNAi flies (arrowheads in panels L8d Normal M) was suppressed by retinoid deprivation (R-free M). Scale bars, 20 μm. ***C***, Top panels, Immunoblotting of adult head lysates collected from *gfp*-RNAi/*gfp*-RNAi and *Ppt1*-RNAi/*Ppt1*-RNAi flies. Flies were treated and immunoblotting was performed as shown in Figure 8*B*. Bottom panel, Statistical analysis of TUNEL-positive nuclei. The percentage of TUNEL-positive nuclei from the apical surface to the retinal floor (indicated by asterisks in the merged images) was calculated as in Figure 1*Ci*. The values are the mean ± SD. ***$p < 0.001$, *t* test. ***D***, Left, Flies were dark-reared or light-exposed (4000 lux) for 4 d, and the dissected retinas were triply stained (Rh1, Cad, and phalloidin). Impaired ommatidia (arrows) were detected in *Psd*-RNAi/*Ppt1*-RNAi retinas. Scale bars, 20 μm. Right, Statistical analysis of the disruption in the retinas of double-knockdown *Psd* and *Ppt1* flies. The percentage of disrupted ommatidia per slice was calculated as shown in Figure 4*D*. Values are the mean ± SD. ***$p < 0.001$, *t* test.

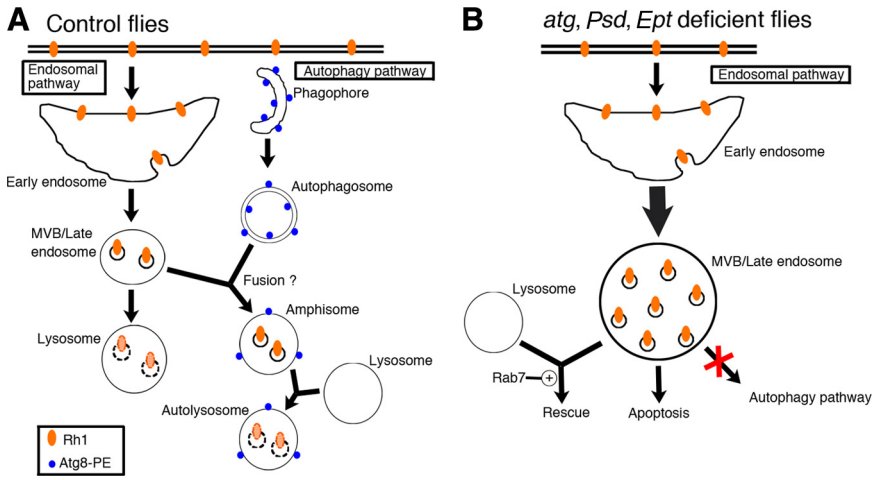

Figure 12. A schematic model of the cross talk between the endosomal and autophagy pathways during light-induced Rh1 degradation. ***A***, In control flies, Rh1 is internalized and degraded by the endosomal pathway (left). The autophagy pathway (right) plays a compensatory role during Rh1 degradation, possibly through the fusion of autophagosomes with Rh1-positive MVB/late endosomes. ***B***, In *atg7-*, *atg8a-*, *Psd-*, or *Ept*-deficient flies, autophagosome formation is impaired. This causes the accumulation of Rh1 in MVB/late endosomes after light exposure as evidenced by the impairment of the divergent pathway shown in ***A***. The Rh1 accumulation in MVB/late endosomes eventually leads to photoreceptor cell death/apoptosis, and this can be suppressed by the overexpression of Rab7, which promotes late endosome to lysosome trafficking.

down flies in this study. However, an Ept knockdown, which reduced PE production, but did not affect mitochondrial function, also showed light-dependent retinal degeneration. Moreover, the morphology of mitochondria in the photoreceptor cells of dark-reared *Psd* knockdown flies appeared normal in our electron-microscopic analyses and the membrane potential was normal in these ommatidia even after light exposure for 2.5 d. Therefore, these results strongly suggested that the *Psd* knockdown causes retinal degeneration through defective PE production and autophagy, rather than through mitochondrial defects.

The retinal degeneration phenotype in *Psd* or *Ept* knockdown flies was rescued when Rh1 expression was reduced in a *ninaE* mutant background, or under retinoid-free conditions. Moreover, exposure to blue light followed by red light exposure blocked the internalization of Rh1 and suppressed the retinal degeneration phenotype in the *Psd* knockdown eyes. These results strongly supported the notion that the intracellular accumulation of Rh1 is the cause of the retinal degeneration in these flies.

A very recent study by Wang et al. (2009) has shown, independently, that light-dependent retinal degeneration is induced by the hyperactivation of target of rapamycin (TOR) protein kinase, or by an *atg7* mutation. The authors also found that inhibition of TOR or inducing Atg1 expression suppressed both the retinal degeneration caused by ectopic expression of the mutant Huntingtin protein (which carries a long polyQ stretch) and phospholipase C (*norpA*)-mediated accumulation of the cytoplasmic rhodopsin–arrestin complex. However, it remains unclear whether autophagy is required for the suppression of polyQ- or *norpA*-induced retinal degeneration. It is also unclear whether rhodopsin is degraded directly by the autophagosome/autolysosome. In this study, we found that Rh1 is required for light-induced retinal degeneration in *Psd* knockdown flies and that Rh1 is incorporated into the autophagosome in normal photoreceptor cells. These results clearly indicate that rhodopsin is degraded through autophagy and is a key target of the autophagy-dependent degradation responsible for the suppression of retinal degeneration.

The processes involved in autophagosome formation, revealed by studies using yeast and mammalian cells, appear to be conserved in *Drosophila*. For example, *Drosophila atg7* and *atg3* mutations produce a significant reduction in the number and size of autophagosomes/autolysosomes in larval fat bodies and midgets (Juhász et al., 2003, 2007), a phenomenon also seen in yeast mutants and mammalian cells (Nakatogawa et al., 2007; Sou et al., 2008). However, the significance of the conjugation of PE to Atg8 had not been directly represented in *Drosophila*. Our study shows that the knockdown of *Psd* impaired both PE-Atg8 conjugation and autophagosome formation, providing direct evidence that PE conjugation to Atg8 is essential for autophagosome formation in *Drosophila*. Moreover, we found that the amount of PE-Atg8 was elevated by exposure to light in *Drosophila* photoreceptor cells. This light-induced formation of autophagosomes has also been reported in rat photoreceptor cells (Remé et al., 1999), suggesting that light-dependent regulation of autophagy in photoreceptor cells may be conserved in metazoa.

The endosomal/lysosomal pathway is necessary for autophagy-dependent degradation, since autophagosomes must fuse to late endosomes (and to MVBs and lysosomes). Defects in the endosomal/lysosomal pathway do indeed hamper autophagy-dependent degradation (Shirahama et al., 1997; Nara et al., 2002; Besteiro et al., 2006; Filimonenko et al., 2007; Lee et al., 2007; Rusten et al., 2007); however, it was unknown whether defects in the autophagic pathway also affected the endosomal degradation pathway. In this study, the mutation and/or knockdown of *atg*, *Psd*, and *Ept* caused the abnormal accumulation of Rh1 in the Rab7-positive late endosome (Fig. 12). On exposure to light, increased amounts of Rh1 are transported to the late endosome and MVBs. In addition to conventional lysosomal activities, this excess Rh1 may also be degraded by autolysosomes that fuse to the late endosome or MVBs, since Rh1 was detected in Atg8b-GFP-positive autolysosomes after light exposure. These results suggested that autophagy plays an essential role in rhodopsin degradation in cooperation with the endosomal degradation pathway. It will be interesting, in future studies, to determine how this compensatory degradation pathway is selected under stress conditions or in pathological contexts.

Insight into INCL, a disease caused by *Ppt1* mutation

INCL is caused by mutations in the *Ppt1* gene (Vesa et al., 1995), which encodes the soluble lysosomal enzyme, Ppt1, and is known to interact genetically with the *Psd* gene (Buff et al., 2007). The pathological features of INCL manifest as normal early development in the first year followed by various neural defects, including blindness (Haltia et al., 1973). However, it is not clear how the loss of Ppt1 activity causes retinal degeneration. It has been reported that *Ppt1* and *Psd* interact genetically when they are overexpressed (Buff et al., 2007). Moreover, in this study, we have demonstrated that *Ppt1* mutants show light-dependent retinal degeneration and that there is a genetic interaction between these genes when they are downregulated. Interestingly, the *Ppt1* knock-out mouse exhibits lysosomal dysfunction (Virmani et al., 2005). Since retinal degeneration in the *Psd* knockdown fly is caused by the intracellular accumulation of rhodopsins, this may also underlie the retinal degeneration that occurs in *Drosophila* and humans as a result of a *Ppt1* disruption. A severe form of

human autosomal dominant retinitis pigmentosa is caused by Arg135 mutant rhodopsins that accumulate in aberrant endosomes (Chuang et al., 2004). It will thus be necessary in future studies to determine whether rhodopsins also accumulate in the photoreceptor cells of INCL patients.

In summary, this study underlines the importance of the interplay between the autophagic and endosomal/lysosomal pathways in protecting light-induced retinal degeneration through the efficient degradation of activated rhodopsin. In addition, we have provided genetic evidence that the autophagic pathway influences the degenerative defects caused by *Ppt1*, although the mechanism is unclear. This report will help to shed light on the mechanisms behind human retinal degenerative diseases, since it is possible that cross talk between the autophagic and endosomal/lysosomal pathways might also be conserved in humans.

References

Acharya JK, Dasgupta U, Rawat SS, Yuan C, Sanxaridis PD, Yonamine I, Karim P, Nagashima K, Brodsky MH, Tsunoda S, Acharya U (2008) Cell-nonautonomous function of ceramidase in photoreceptor homeostasis. Neuron 57:69–79.

Alloway PG, Howard L, Dolph PJ (2000) The formation of stable rhodopsin-arrestin complexes induces apoptosis and photoreceptor cell degeneration. Neuron 28:129–138.

Amar N, Lustig G, Ichimura Y, Ohsumi Y, Elazar Z (2006) Two newly identified sites in the ubiquitin-like protein Atg8 are essential for autophagy. EMBO Rep 7:635–642.

Besteiro S, Williams RA, Morrison LS, Coombs GH, Mottram JC (2006) Endosome sorting and autophagy are essential for differentiation and virulence of *Leishmania major*. J Biol Chem 281:11384–11396.

Brown SV, Hosking P, Li J, Williams N (2006) ATP synthase is responsible for maintaining mitochondrial membrane potential in bloodstream form *Trypanosoma brucei*. Eukaryot Cell 5:45–53.

Buff H, Smith AC, Korey CA (2007) Genetic modifiers of *Drosophila* palmitoyl-protein thioesterase 1-induced degeneration. Genetics 176:209–220.

Chinchore Y, Mitra A, Dolph PJ (2009) Accumulation of rhodopsin in late endosomes triggers photoreceptor cell degeneration. PLoS Genet 5:e1000377.

Choi JY, Wu WI, Voelker DR (2005) Phosphatidylserine decarboxylases as genetic and biochemical tools for studying phospholipid traffic. Anal Biochem 347:165–175.

Chuang JZ, Vega C, Jun W, Sung CH (2004) Structural and functional impairment of endocytic pathways by retinitis pigmentosa mutant rhodopsin-arrestin complexes. J Clin Invest 114:131–140.

Entchev EV, Schwabedissen A, González-Gaitán M (2000) Gradient formation of the TGF-beta homolog Dpp. Cell 103:981–991.

Filimonenko M, Stuffers S, Raiborg C, Yamamoto A, Malerød L, Fisher EM, Isaacs A, Brech A, Stenmark H, Simonsen A (2007) Functional multivesicular bodies are required for autophagic clearance of protein aggregates associated with neurodegenerative disease. J Cell Biol 179:485–500.

Glaser RL, Hickey AJ, Chotkowski HL, Chu-LaGraff Q (2003) Characterization of *Drosophila* palmitoyl-protein thioesterase 1. Gene 312:271–279.

Haltia M, Rapola J, Santavuori P (1973) Infantile type of so-called neuronal ceroid-lipofuscinosis. Histological and electron microscopic studies. Acta Neuropathol 26:157–170.

Hara T, Nakamura K, Matsui M, Yamamoto A, Nakahara Y, Suzuki-Migishima R, Yokoyama M, Mishima K, Saito I, Okano H, Mizushima N (2006) Suppression of basal autophagy in neural cells causes neurodegenerative disease in mice. Nature 441:885–889.

Hardie RC (1991) Voltage-sensitive potassium channels in *Drosophila* photoreceptors. J Neurosci 11:3079–3095.

Hartong DT, Berson EL, Dryja TP (2006) Retinitis pigmentosa. Lancet 368:1795–1809.

Hickey AJ, Chotkowski HL, Singh N, Ault JG, Korey CA, MacDonald ME, Glaser RL (2006) Palmitoyl-protein thioesterase 1 deficiency in *Drosophila melanogaster* causes accumulation of abnormal storage material and reduced life span. Genetics 172:2379–2390.

Juhász G, Csikós G, Sinka R, Erdélyi M, Sass M (2003) The *Drosophila* homolog of Aut1 is essential for autophagy and development. FEBS Lett 22:154–158.

Juhász G, Erdi B, Sass M, Neufeld TP (2007) Atg7-dependent autophagy promotes neuronal health, stress tolerance, and longevity but is dispensable for metamorphosis in *Drosophila*. Genes Dev 21:3061–3066.

Kanehisa M, Araki M, Goto S, Hattori M, Hirakawa M, Itoh M, Katayama T, Kawashima S, Okuda S, Tokimatsu T, Yamanishi Y (2008) KEGG for linking genomes to life and the environment. Nucleic Acids Res 36:D480–D484.

Karan S, Zhang H, Li S, Frederick JM, Baehr W (2008) A model for transport of membrane-associated phototransduction polypeptides in rod and cone photoreceptor inner segments. Vision Res 48:442–452.

Kirisako T, Ichimura Y, Okada H, Kabeya Y, Mizushima N, Yoshimori T, Ohsumi M, Takao T, Noda T, Ohsumi Y (2000) The reversible modification regulates the membrane-binding state of Apg8/Aut7 essential for autophagy and the cytoplasm to vacuole targeting pathway. J Cell Biol 151:263–276.

Kiselev A, Socolich M, Vinós J, Hardy RW, Zuker CS, Ranganathan R (2000) A molecular pathway for light-dependent photoreceptor apoptosis in *Drosophila*. Neuron 28:139–152.

Knust E (2007) Photoreceptor morphogenesis and retinal degeneration: lessons from *Drosophila*. Curr Opin Neurobiol 17:541–547.

Komatsu M, Waguri S, Chiba T, Murata S, Iwata J, Tanida I, Ueno T, Koike M, Uchiyama Y, Kominami E, Tanaka K (2006) Loss of autophagy in the central nervous system causes neurodegeneration in mice. Nature 441:880–884.

Lee JA, Beigneux A, Ahmad ST, Young SG, Gao FB (2007) ESCRT-III dysfunction causes autophagosome accumulation and neurodegeneration. Curr Biol 17:1561–1567.

Michaelides M, Hardcastle AJ, Hunt DM, Moore AT (2006) Progressive cone and cone-rod dystrophies: phenotypes and underlying molecular genetic basis. Surv Ophthalmol 51:232–258.

Naito Y, Yamada T, Matsumiya T, Ui-Tei K, Saigo K, Morishita S (2005) dsCheck: highly sensitive off-target search software for double-stranded RNA-mediated RNA interference. Nucleic Acids Res 33:W589–W591.

Nakatogawa H, Ichimura Y, Ohsumi Y (2007) Atg8, a ubiquitin-like protein required for autophagosome formation, mediates membrane tethering and hemifusion. Cell 130:165–178.

Nara A, Mizushima N, Yamamoto A, Kabeya Y, Ohsumi Y, Yoshimori T (2002) SKD1 AAA ATPase-dependent endosomal transport is involved in autolysosome formation. Cell Struct Funct 27:29–37.

Nebauer R, Rosenberger S, Daum G (2007) Phosphatidylethanolamine, a limiting factor of autophagy in yeast strains bearing a defect in the carboxypeptidase Y pathway of vacuolar targeting. J Biol Chem 282:16736–16743.

Nishihara S, Ueda R, Goto S, Toyoda H, Ishida H, Nakamura M (2004) Approach for functional analysis of glycan using RNA interference. Glycoconj J 21:63–68.

Orem NR, Dolph PJ (2002a) Loss of the phospholipase C gene product induces massive endocytosis of rhodopsin and arrestin in *Drosophila* photoreceptors. Vision Res 42:497–505.

Orem NR, Dolph PJ (2002b) Epitope masking of rhabdomeric rhodopsin during endocytosis-induced retinal degeneration. Mol Vis 8:455–461.

Orem NR, Xia L, Dolph PJ (2006) An essential role for endocytosis of rhodopsin through interaction of visual arrestin with the AP-2 adaptor. J Cell Sci 119:3141–3148.

Pandey UB, Nie Z, Batlevi Y, McCray BA, Ritson GP, Nedelsky NB, Schwartz SL, DiProspero NA, Knight MA, Schuldiner O, Padmanabhan R, Hild M, Berry DL, Garza D, Hubbert CC, Yao TP, Baehrecke EH, Taylor JP (2007) HDAC6 rescues neurodegeneration and provides an essential link between autophagy and the UPS. Nature 447:859–863.

Picking WL, Chen DM, Lee RD, Vogt ME, Polizzi JL, Marietta RG, Stark WS (1996) Control of *Drosophila* opsin gene expression by carotenoids and retinoic acid: Northern and Western analyses. Exp Eye Res 63:493–500.

Raghu P, Usher K, Jonas S, Chyb S, Polyanovsky A, Hardie RC (2000) Constitutive activity of the light-sensitive channels TRP and TRPL in the *Drosophila* diacylglycerol kinase mutant, rdgA. Neuron 26:169–179.

Remé CE, Wolfrum U, Imsand C, Hafezi F, Williams TP (1999) Photoreceptor autophagy: effects of light history on number and opsin content of degradative vacuoles. Invest Ophthalmol Vis Sci 40:2398–2404.

Rusten TE, Vaccari T, Lindmo K, Rodahl LM, Nezis IP, Sem-Jacobsen C, Wendler F, Vincent JP, Brech A, Bilder D, Stenmark H (2007) ESCRTs and Fab1 regulate distinct steps of autophagy. Curr Biol 17:1817–1825.

Schapira AH (2008) Mitochondrial dysfunction in neurodegenerative diseases. Neurochem Res 33:2502–2509.

Scott RC, Schuldiner O, Neufeld TP (2004) Role and regulation of starvation-induced autophagy in the *Drosophila* fat body. Dev Cell 7:167–178.

Seto ES, Bellen HJ, Lloyd TE (2002) When cell biology meets development: endocytic regulation of signaling pathways. Genes Dev 16:1314–1336.

Shirahama K, Noda T, Ohsumi Y (1997) Mutational analysis of Csc1/Vps4p: involvement of endosome in regulation of autophagy in yeast. Cell Struct Funct 22:501–509.

Sou YS, Waguri S, Iwata J, Ueno T, Fujimura T, Hara T, Sawada N, Yamada A, Mizushima N, Uchiyama Y, Kominami E, Tanaka K, Komatsu M (2008) The Atg8 conjugation system is indispensable for proper development of autophagic isolation membranes in mice. Mol Biol Cell 19:4762–4775.

Steenbergen R, Nanowski TS, Beigneux A, Kulinski A, Young SG, Vance JE (2005) Disruption of the phosphatidylserine decarboxylase gene in mice causes embryonic lethality and mitochondrial defects. J Biol Chem 280:40032–40040.

Sun Q, Fan W, Chen K, Ding X, Chen S, Zhong Q (2008) Identification of Barkor as a mammalian autophagy-specific factor for Beclin 1 and class III phosphatidylinositol 3-kinase. Proc Natl Acad Sci U S A 105:19211–19216.

Tekinay T, Wu MY, Otto GP, Anderson OR, Kessin RH (2006) Function of the *Dictyostelium discoideum* Atg1 kinase during autophagy and development. Eukaryot Cell 5:1797–1806.

Todde V, Veenhuis M, van der Klei IJ (2009) Autophagy: principles and significance in health and disease. Biochim Biophys Acta 1792:3–13.

Vance JE (2008) Phosphatidylserine and phosphatidylethanolamine in mammalian cells: two metabolically related aminophospholipids. J Lipid Res 49:1377–1387.

Venkatachalam K, Long AA, Elsaesser R, Nikolaeva D, Broadie K, Montell C (2008) Motor deficit in a *Drosophila* model of mucolipidosis type IV due to defective clearance of apoptotic cells. Cell 135:838–851.

Vesa J, Hellsten E, Verkruyse LA, Camp LA, Rapola J, Santavuori P, Hofmann SL, Peltonen L (1995) Mutations in the palmitoyl protein thioesterase gene causing infantile neuronal ceroid lipofuscinosis. Nature 376:584–587.

Virmani T, Gupta P, Liu X, Kavalali ET, Hofmann SL (2005) Progressively reduced synaptic vesicle pool size in cultured neurons derived from neuronal ceroid lipofuscinosis-1 knockout mice. Neurobiol Dis 20:314–323.

Wang T, Lao U, Edgar BA (2009) TOR-mediated autophagy regulates cell death in *Drosophila* neurodegenerative disease. J Cell Biol 186:703–711.

Webel R, Menon I, O'Tousa JE, Colley NJ (2000) Role of asparagine-linked oligosaccharides in rhodopsin maturation and association with its molecular chaperone, NinaA. J Biol Chem 275:24752–24759.

Xu H, Lee SJ, Suzuki E, Dugan KD, Stoddard A, Li HS, Chodosh LA, Montell C (2004) A lysosomal tetraspanin associated with retinal degeneration identified via a genome-wide screen. EMBO J 23:811–822.

Yano H, Yamamoto-Hino M, Abe M, Kuwahara R, Haraguchi S, Kusaka I, Awano W, Kinoshita-Toyoda A, Toyoda H, Goto S (2005) Distinct functional units of the Golgi complex in *Drosophila* cells. Proc Natl Acad Sci U S A 102:13467–13472.